



## Research papers

# Estimation of water turbidity and analysis of its spatio-temporal variability in the Danube River plume (Black Sea) using MODIS satellite data

Sorin Constantin <sup>a,\*</sup>, David Doxaran <sup>b</sup>, Ştefan Constantinescu <sup>a</sup><sup>a</sup> University of Bucharest, Faculty of Geography, Romania<sup>b</sup> Laboratoire d'Océanographie de Villefranche, UMR7093, CNRS-UPMC, France

## ARTICLE INFO

## Article history:

Received 11 June 2015

Received in revised form

8 October 2015

Accepted 19 November 2015

Available online 2 December 2015

## Keywords:

Turbidity

MODIS

Black Sea

Danube

## ABSTRACT

Ocean colour remote sensing information brings important insights for monitoring coastal areas. These regions are home to important natural ecosystems and changes that occur here can have important impacts not only on the local environment, but also on connected wetlands or offshore areas. The present study proposes a new regional methodology for water turbidity retrieval using the MODIS red band at 250 m spatial resolution in the Danube Delta coastal area. For this purpose, multiple in-situ turbidity observations were used in order to determine a valid relationship between data collected with turbidity meters and remote sensing reflectance obtained from satellite data. A special attention is given to the atmospheric correction of satellite data, since complex optical waters require adapted methodologies for accurate remote sensing reflectance computation. Based on products derived using the proposed algorithm, the dynamics of turbidity is evaluated for multiple time periods: from local Terra to Aqua overpasses (couple of hours), daily and monthly. Results show a clear strong connection between the Danube discharge and water turbidity in the coastal area. However other environmental parameters (e.g., wind stress) also play an important role and contribute to the magnitude of the river plume extension.

© 2015 Elsevier Ltd. All rights reserved.

## 1. Introduction

Coastal areas are important habitats that can sustain ecosystems for many wildlife flora and fauna. Even if they represent only 7% of the total oceanic area (Gattuso and Smith, 2007), their ecological, social and economic importance is recognized worldwide by the scientific community. They account for about 15% of the oceanic primary production, 50% of total calcium carbonate deposition and 90% of the sedimentary remineralisation (Gattuso and Smith, 2007). Turbidity is one of the main parameters that can be used to evaluate the water quality and also to indirectly determine the amount of suspended sediments (Kemker, 2014) in coastal waters. It represents an optical determination of water clarity. Apart from the fact that turbidity measurements can be used in order to derive concentrations of suspended particles (Dogliotti et al., 2015, Kemker, 2014), it can also be considered as a proxy for water quality, since high values lead to shallow penetration of light. This in turn dictates the photic zone extension and the depth of phytoplankton production. Algal blooms can contribute significantly to turbidity values further offshore (Kemker,

2014), but the amount of total suspended sediments (predominantly inorganic particles) remains the main cause of turbidity close to river mouths. Turbidity can be reported using different measurements units: NTU (Nephelometric Turbidity Unit), FTU (Formazin Turbidity Unit), FNU (Formazin Nephelometric Unit) etc. They are based on same type of calibration using Formazin, a standard scattering solution. Although many consider the above mentioned units to be equivalent, it is important to stress out that turbidity instruments with different designs commonly do not yield identical or equivalent results (Anderson, 2005). Turbidity was chosen as in-situ measurement for two main reasons: obtaining good quality observations is easy since the available instruments are designed as to minimize the influence of human factor on the possible errors of measurement and more important, turbidity is an optical property, compared to TSM, therefore it is strongly connected to the particulate backscattering coefficient ( $b_p$  in  $m^{-1}$ ), thus to remote sensing reflectance (Dogliotti et al., 2015).

By monitoring the dynamics of turbidity values, conclusions can be drawn not only for the marine areas themselves, but also for wetlands associated with them. Deltas can continue to exist only if solid river discharge rates remain unchanged in order to overcome sand and mud washing by waves and currents (Giosan et al., 2014). The Danube Delta is a well preserved wetland, with numerous channels, lakes, marshes and dunes. New studies have

\* Corresponding author.

E-mail address: [sorin.c.geo@gmail.com](mailto:sorin.c.geo@gmail.com) (S. Constantin).

highlighted the increased pressure that these types of deltaic areas are facing, due to decreasing sediment inputs as a result of human intervention on rivers courses and deltaic areas and also due to sea level rise at global scale (Giosan et al., 2014). This triggers the necessity to act fast in order to properly restore natural wetlands with the help of improved data collection, modeling and real-time monitoring (Giosan et al., 2014). Decision makers and other stakeholders need to be provided with updated and accurate information on suspended sediments dynamics in order to better address coastal protection works planning. These challenges can be, at least partly, overcome by the use of ocean colour remote sensing information (IOCCG, 2000).

Few attempts have been made to characterize the dynamics of water turbidity and/or total suspended matter concentrations over the Romanian deltaic coastal area. Some of them used remote sensing techniques in conjunction with or to support other methodologies, such as modelling (Stanev and Kandilarov, 2012), others made use of MODIS (Moderate Resolution Imaging Spectroradiometer) true colour images for visual interpretation of the river plume (Ovejanu, 2012), while studies addressing in detail the capabilities of satellite data to study turbidity remain sparse. One good example is the study of Gütler et al., (2013), which uses MERIS (MEdium Resolution Imaging Spectrometer) data to evaluate the turbidity dynamics in the Romanian coastal area, based on an algorithm developed and tested using in-situ turbidity determination from other geographical areas (Gohin, 2011), with turbidity computed as a factor of non algal (mineral) suspended particulate matter and chlorophyll concentrations. Further, the obtained products were validated using few Secchi disk measurements.

Our present study represents a distinct and innovative approach to the turbidity analysis in the Danube Delta coastal area, by making

full use of the spatial resolution, and in some degree of spectral resolution, of MODIS products in conjunction with reliable in-situ measurements of turbidity. Atmospheric correction issues, of great importance in optical complex coastal waters, are also treated in detail for our area of interest. Other differences between the two approaches refer to the fact that we are proposing long-term composite products that can be used to analyze monthly and seasonal variations in turbidity and we are also making observations on the dynamics at high temporal resolution between Terra and Aqua passes.

Successful efforts in retrieving water turbidity or suspended sediment concentration using remote sensing data or in-situ reflectance determinations in highly and moderately turbid coastal areas have been previously recorded for multiple areas on the Globe, such as the North Sea (Nechad et al., 2010, Ruddick et al., 2003), Gironde estuary (Doxaran et al., 2002, 2006 and 2009), Gulf of Mexico (Chen et al., 2007, Miller and McKee, 2004), Adour River plume (Petus et al., 2010 and 2014) and others. Important studies focused also on multiple study areas at once (Dogliotti et al., 2015), trying to impose a global perspective on a problem that seemed exclusively regional until recently. This is emerging as a valid direction in the study of turbidity, mainly after the evolution of algorithms that could be considered generally valid (Nechad et al., 2009 and 2010). Still, local established relationships between turbidity and remote sensing reflectance can contribute to quality regional analysis and also to the further validation of the global algorithms.

### 1.1. General characteristics of the study area

The area of interest (AOI) for the present study is represented by the coastal zone in front of Danube Delta (Fig. 1). It is characterized by shallow waters, with maximum depths of around

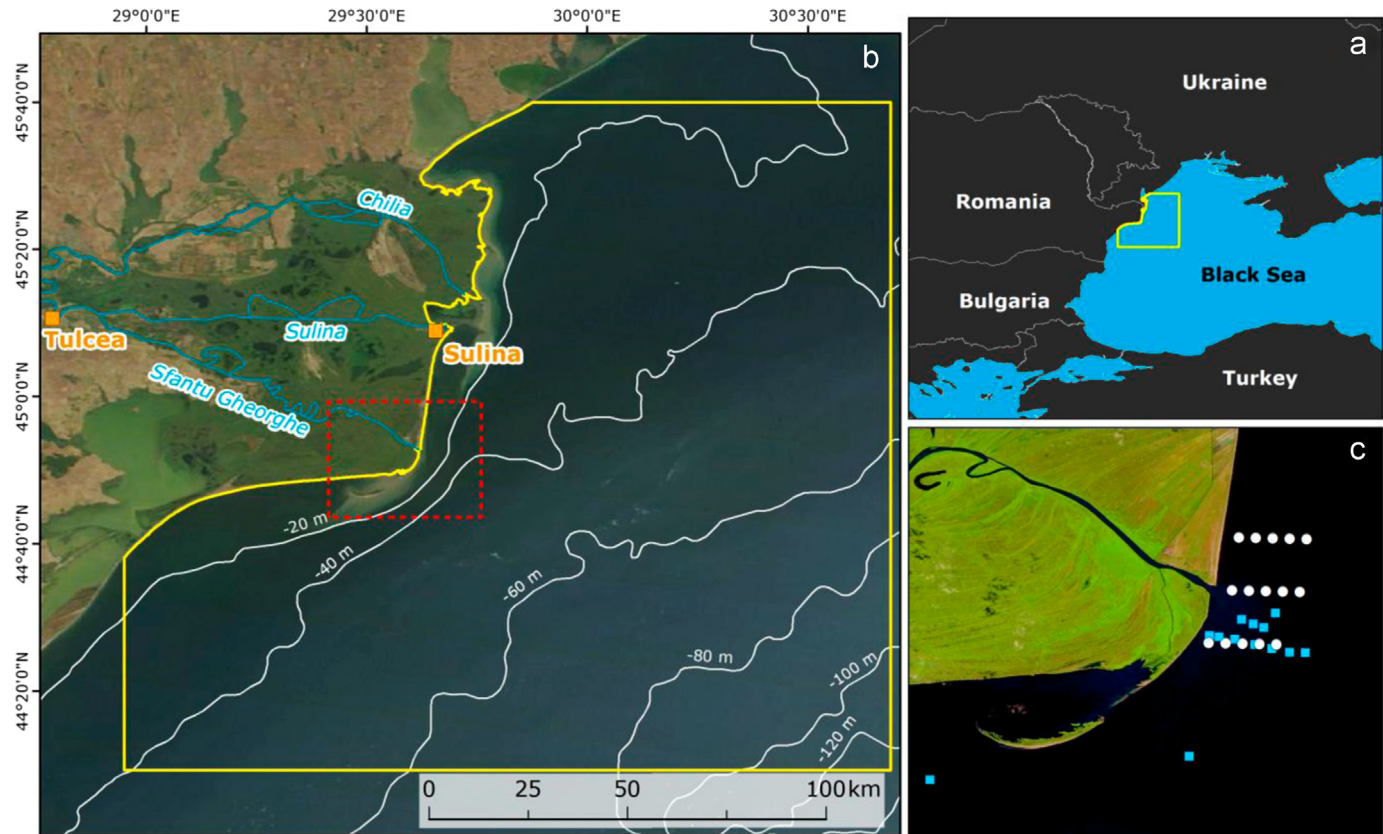


**Fig. 1.** a) Regional localization of the area of interest (AOI); b) Delimitation of AOI (background image: MODIS Terra natural colour composite); c) Sfântu Gheorghe river mouth and turbidity in-situ measurements locations (white circles represent regular sampling points in different field campaigns, from 2013 and 2014, and blue rectangles are other individual measurements, acquired in 2008; background image: Landsat 8 natural colour composite). (For interpretation of the references to color in this figure legend, the reader is referred to the web version of this article.)

120 m in the South-Eastern part. From this point of view, the area is very similar to the entire North-Western Black Sea basin, which is highly dominated by river inputs from rivers such as Dnieper, Bug, Dniester and especially Danube. The last one accounts for approximately 60% of the total river input into the North-Western continental shelf (Popa, 1993; Staney and Kandilarov, 2012). Pollution, inadequate agricultural practices and hydro-technical works (dikes, dams, etc) on the main rivers courses have led to an increased pressure on the biocenosis over the last decades. This in turn translated into more intense eutrophication processes and loss of fish stocks (Panin et al., 1998). The AOI is a micro-tidal zone, with a tide amplitude of just up to 0.12 m (Bondar et al., 2011), therefore with a low impact on sediment resuspension and consequently turbidity values.

Wind conditions on the Danube Delta coastal area are almost invariant from the Northern to the Southern limit, since the coast is relatively short. Average annual wind speeds are between 5 and 6.5 m/s, with a predominant North-East direction (Giosan et al., 1999). For the purpose of our study, data measured at Sulina meteorological station was used, since the station is situated on the jetties at the river mouth, therefore more suited for coastal analysis than other observations acquired more in-land.

The regional circulation is dominated by the presence of a long-shore current along the coastline, stronger in wintertime. In the absence of winds, these currents are formed by the difference in salinity induced by the Danube freshwater discharge (Dinu et al., 2011). Otherwise, the flow is mainly influenced by the predominant winds, therefore it is oriented in South-West direction, with the possibility to change direction during periods when wind is blowing from the opposite side, especially in the warm season (Dinu et al., 2011).

Since the AOI is part of the North-Western basin of the Black Sea, it is highly influenced by the large amount of total freshwater input from all the rivers in the region, Danube being the most important. This influences the primary production, with consequences that spread at the level of the entire basin, with maximum production occurring in spring (mainly diatoms) and autumn (dominated by cocolithophorids) (Sorokin, 1983; Sur et al., 1996). The entire Black Sea is a moderate to high productivity region (Koblenz-Mishke et al., 1970), with other episodic blooms occurring, apart from the two cyclic ones mentioned already. Such non-regular blooms are dominated by cocoliths and dinoflagellates appearing in coastal areas. Other important phenomena are spring and summer development of red tides (dinoflagellates), especially on the Romanian coast (Tumantseva, 1985).

In the close proximity of the shore, the sedimentary and ecological status is heavily controlled by the fluxes from the Danube branches, but further away offshore, this dominance decreases and organic matter contribution is more present. In fact, at the level of the entire Black Sea basin, annual production of organic matter ( $818 \times 10^6$  t year $^{-1}$ ) exceeds the total sediment load brought by the rivers ( $150 \times 10^6$  t year $^{-1}$ ) (Staney and Kandilarov, 2012). In the present AOI, the river plume is mainly overlapping the extent of plankton production area and organic contribution to turbidity values is limited, but this still requires more evidence (Güttler et al., 2013).

Danube sediment inputs significantly influence the turbidity dynamics in the coastal area, therefore modifications along its course can have an indirect impact at the river mouth. Important hydrotechnical works have been conducted along the Danube River and its three branches, Chilia, Sulina and Sfântu Gheorghe, since the middle of the 19th century (Bondar et al., 2011; Budileanu, 2013; Constantinescu et al., 2010). Among these works, it is important to mention the numerous dams that led to a dramatic decrease in solid discharge at the river mouths. Figures tend to vary from one author to another, but the general accepted amount is a 60% loss in sediment discharge (McCarney-Castle et al., 2012).

Other activities included navigation wise works (dredging, channel cutting for reed exploitation and fisheries etc), which modified the hydrological balance between the three main branches.

Loss of sediment discharge from the Danube translates into accelerated coastal erosion (Giosan, 1998; Vespremeanu, 2007; Stanica and Panin, 2009), with important beach size reduction that heavily impacts touristic activities. Other consequences include a reduction in sedimentation rates in the deltaic area, which can increase its vulnerability to floods in the context of global sea level rise (Giosan et al., 2013).

When analyzing the river plume dynamics, it is important to take into consideration the behavior of the water masses at the interface between river and sea. In the case of the Danube, the most frequent scenario is hypopycnal conditions, with lower density river waters floating over the denser marine ones (Wright, 1977). These differences in density are mainly driven by differences in salinity. The hypopycnal flow conditions can lead to large river plume extensions offshore, meaning sediments are transported for a larger distance before they are deposited (Ovejanu, 2012). The stratification of water masses was reported also locally for the Sulina river mouth by Bondar et al. (2011).

Previous studies have concluded that for explaining the dynamics of coastal turbidity it is important to have a good understanding on the river discharge status, but also on other factors, such as phytoplankton development, meteorological conditions or sediment resuspension (Güttler et al., 2013). The same study attempts an integrated approach for deltaic-coastal areas, therefore the turbidity analysis for the marine zone is limited to fewer images and specific case studies than the present paper. A good temporal density of satellite data coming from MODIS sensors (onboard the Aqua and Terra platforms) makes the following analysis appropriate for characterization of turbidity dynamics in the Danube Delta coastal area at different time scales.

## 1.2. Objectives

The two main objectives of the present study are:

a) To develop a regional algorithm for turbidity ( $T$ ) retrieval using MODIS datasets. In order to reach this goal, several steps had to be followed. First of all, a robust algorithm for atmospheric correction was selected and tested. Second, MODIS derived remote sensing reflectance ( $R_{rs}$ , sr $^{-1}$ ) and in-situ turbidity measurements are used to derive an equation that can translate  $R_{rs}$  into  $T$ . Third, both 250 m spatial resolution MODIS bands, one in the red and the other in the near-infrared (NIR) spectral regions, were evaluated in order to determine the most suited methodology for  $T$  retrieval in the Danube Delta coastal area.

b) To make hourly, daily and monthly variation analyses for  $T$ , over two consecutive years (2013 and 2014). This specific time period was chosen due to the availability of necessary data (in-situ  $T$  measurements, remote sensing products, Danube liquid and solid discharges). Only two years were analyzed since the primary purpose is to evaluate the utility of turbidity derived from our regional algorithm to study local characteristics and dynamics.

The section of the paper dedicated to presenting the datasets used for the analysis and the methodology shall address all the necessary theoretical issues. The “Results and Discussions” part envelopes all the findings of the current study, in correlation with the specified objectives, starting with the atmospheric correction procedure using three different algorithms, up to inversion of  $R_{rs}$  measurements to turbidity values and generation of final maps and graphics that reflect the dynamics of turbidity at different time scales: hourly, daily and monthly. This section is also reserved for observations on the overall quality of the proposed methodology and the findings of the study and finally, conclusions are drawn.

## 2. Data and methods

The present study combines in-situ turbidity measurements and match-ups with satellite-derived remote sensing reflectance observations in order to establish a methodology to derive water turbidity using satellite data.

Turbidity can be defined as an optical property of a liquid mainly caused by light scattering and to some extent by light absorption along the photons pathlength (Anderson, 2005). Basically, the turbidity of water is directly connected to the amount of light scattered by particles in suspension in the water and therefore dictates the clarity of a water column. Robust relationships can be established between turbidity and the concentration of total suspended matter, but these relationships are also affected by the size distribution of suspended particles. Turbidity does not represent an exact measurement of the concentration of suspended solids in the water sampled, but is a good indirect indicator for it (Kemker, 2014). The measurement unit used in this paper for turbidity is FTU (Formazin Turbidity Units). For water quality monitoring, turbidity was listed as a primary parameter to be measured by the European Union (2008).

The MODIS satellite sensor is an ocean colour compatible instrument capable of measuring the radiometric flux from the Earth surface passing through the atmosphere and reaching the sensor at multiple bands in the wavelengths ranging from visible to near infrared domain of the electromagnetic spectrum. The colour of the water (determined by illumination conditions and in-water optically-active constituents) is defined by the spectral variations of the remote sensing reflectance signal ( $R_{rs}$ , in  $\text{sr}^{-1}$ ), which is the ratio between the water-leaving radiance and the downwelling irradiance just above the sea-air interface (Mobley, 1999). By opposition the irradiance seawater reflectance ( $R$ , dimensionless) is the ratio between the upwelling and downwelling irradiance, usually ignoring the water-leaving directional effects.

The methodology adopted in the present study relies on obtaining quality  $R_{rs}$  products from both MODIS Aqua and Terra satellite data by applying adequate processing techniques. The most important step is related to atmospheric correction and therefore this part is given a special attention. Based on the  $R_{rs}$  information, turbidity products are then obtained, which are further used in spatial analysis in order to determine the daily and monthly dynamics. We are using MODIS datasets because it provides two images per day (depending on cloud cover) of the whole AOI at an appropriate spatial resolution (250 m). Also, users have access to a large archive (more than 12 years) of data and MODIS capabilities in analyzing turbidity in coastal areas was already proven by multiple studies (Doxaran et al., 2009, Miller and McKee, 2004, Petus et al., 2010, Petus et al., 2014), and, above all, MODIS is still in operation, which makes it the most suited sensor to be used in operational monitoring of the coastal areas.

### 2.1. In-situ measurements

In-situ turbidity measurements were collected using a HI 98713 turbidity meter (Hanna Instruments), during multiple field

campaigns, near Sfântu Gheorghe Danube River mouth. In the case of 2013 and 2014 campaigns, measurements were collected along three predefined transects, approximately 4 km apart from each other and with a distance between points of roughly 1 km (white dots in Fig. 1(c)). Water samples were collected from the upper layers of the water column (first 10 cm) and multiple readings were performed before the final value was stored. Good practices described in Anderson (2005) were followed during all field campaigns. The turbidity meter used has the capability of measuring turbidity in Formazin Turbidity Units (FTU) over the range 1–1000. It can provide reliable and accurate readings for low turbidity values. The HI 98713 meets the requirements of the ISO 7027 for water quality. The optical system includes a near-infrared light source ( $\lambda=860 \text{ nm}$ ), a scattered light detector ( $90^\circ$ ) and a transmitted light detector ( $180^\circ$ ). The measurements are based on the ratio of the signals from the two detectors. The used algorithm corrects and compensates for interferences of colour, making the HI 98713 turbidity meter colour-compensated (according to HI 98713 Instruction Manual).

A total of 89 in-situ turbidity observations were initially available (field campaigns undertaken in August 2008, July 2013 and August 2014). Using these, 62 match-ups with MODIS derived  $R_{rs}$  were established (the remaining 26 measurements fall inside areas where the computation of  $R_{rs}$  is not possible or very difficult, as too close to the shoreline or even on interior delta canals). A further step was to filter these 62  $R_{rs}$ -T pairs based on the magnitude of contamination due to land or clouds proximity or other interfering factors. Basically, pairs that fall too close to land and might be affected by stray light were discarded. This step was performed even for pixels that were not flagged as affected after processing the data, but following a visual inspection it was concluded that high reflectance values might have other contributions except high particulate concentration. Another decision factor for discarding pairs of data was the positioning in areas with very high dynamics in terms of spectral response and, also, close to pixels edge. Minor geo-referencing issues might have resulted in false coupling between in-situ turbidity and remote sensing reflectance values. Therefore, it was decided not to take into account these situations. Finally, 44 pairs (Table 1) were selected as good quality information to be used further.

The turbidity in-situ observations cover a significant range of values, from 1.8 FTU up to almost 160 FTU, which guarantees that a wide variety of possible conditions are covered. It is also to be noticed that, apart from the field campaign undertaken on 2nd of August 2008, the rest of turbidity measurements were generally lower than 60 FTU. As we shall further see, this reflects the normal conditions in our AOI, high turbidity values being observed only during very limited time periods. Also, exceptional high turbidity values recorded were observed very close to the coastline, when the Danube sediment discharge had extremely high values (during spring floods). It is expected that further offshore, where dilution of the river is higher, the values of turbidity will be much lower. This occurs in normal and even high solid river discharge conditions.

Other in-situ measurements used in the context of this study are water level values for the Danube River collected at Tulcea

**Table 1**

Details on in-situ measurements. Match-ups are formed by valid pairs of in-situ turbidity measurements and satellite derived remote sensing reflectance values.

Day	Hourly interval for data collection (UTC)	Time of acquisition for satellite data used (UTC)	Number of match-ups with MODIS $R_{rs}$	Minimum FTU	Maximum FTU
30-Aug-14	06:00–10:30	8:35	15	3.5	66.5
14-Aug-14	10:00–12:20	10:20	6	15.3	32.1
30-Jul-13	10:00–13:00	11:30	8	1.8	5.6
13-Aug-08	06:00–09:00	8:35	4	2.9	7.6
2-Aug-08	06:25–10:20	8:55	11	3.8	159

hydrological station, situated upstream Danube River, at the entrance into Danube Delta. Since we found out that there is a very high correlation (determination coefficient close to 1; work not presented in this paper) between the river liquid discharge and water level for several years (2010–2013), and since the second type of measurements are more frequent, we decided to present water levels for our analysis. The same very good correlation between liquid discharge and water level was signaled also by other studies. Gütler et al., (2013) found the determination coefficient to be  $r^2=0.97$  for Ceatal Izmail station (placed at the Delta apex) for the period 1932–2008, while Bondar and Panin (2001) discussed into more detail this correlation.

There are important differences between the two years analysed (Fig. 2). In 2013, high water levels in the first part of the year are more pronounced than in 2014, while for both years the average in this period is still above the multiannual (1941–2011) monthly average. In 2013 the water levels are 31% higher than the average for the time period March–June, while in 2014 higher levels (more than 23% compared to the multiannual average) can be observed in May–June. Another difference between 2013 and 2014, concerns the months of August and September. While in the first case the water levels are under the average, for 2014 they reflect abnormal high values.

Hourly wind speed and direction measurements were also necessary for analyzing the turbidity dynamics in the Danube Delta coastal area. These observations were acquired for Sulina meteorological station for all the days with cloud-free satellite data from 2013 and 2014. Data was available through the Ogimet service (<http://www.ogimet.com>) which uses mainly NOAA (National Oceanic and Atmospheric Administration) services to redistribute meteorological information.

## 2.2. Satellite data

Remote sensing data represents the only technique available today able to give a synoptic overview of the turbidity dynamics over large coastal areas. However it is important to mention that remote sensing data can be used to retrieve sub-surface turbidity estimates (the depth depends on several factors such as illumination conditions and in-water constituents concentrations), without the possibility to have an integrated overview of the whole water column. This can be achieved using both forward (using the inherent optical properties of water) and inverse models (computing in-water constituents based on apparent optical properties of water). The methodology described in this paper is going to be based on the second one, by establishing an empirical algorithm.

For the present study, MODIS data recorded aboard both Aqua and Terra satellites was used. In a cloud-free situation, this translates into

two products/images covering the AOI each day, therefore having a high temporal resolution. Although not all 36 spectral bands can be used for ocean colour applications, MODIS offers very good quality products, from radiometric and spectral point of view, to be used in marine analysis. Bands 1 (red, centered at  $\lambda=645$  nm) and 2 (NIR, centred at  $\lambda=859$  nm), at 250 m spatial resolution, are widely used for coastal applications and especially for turbidity and TSM estimations (Miller and McKee, 2004; Doxaran et al., 2009; Petus et al., 2010, 2014). Even though these bands were originally designed for land applications, their usefulness in coastal ocean colour studies was proven over the years, since they have the advantage to not saturate over turbid waters. The downfall is the lower signal-to-noise ratio (SNR) (meaning lower sensitivity), compared with band designed for ocean studies. But, the presence of both near-infrared (NIR) and shortwave-infrared (SWIR) bands for MODIS offers the possibility to explore new atmospheric correction methods (Franz, 2006). For our study we tested both red and NIR bands from the MODIS Aqua and Terra sensors in order to map turbidity. The sensitivity of reflectance at shorter wavebands to low turbidity values compared to high turbidity that are more correlated with longer wavebands (Nechad et al., 2009; Ouillon et al., 2008; Shen et al., 2010), was one of the main criteria used to choose the final band to be used for turbidity retrievals in Danube Delta coastal area. MODIS data is intensively used for oceanographic applications, therefore adapted atmospheric correction algorithms for coastal areas have been developed and were already implemented in specific software packages. Datasets were acquired from NASA's Ocean Biology Processing Group web site (Level 1 A products) and further processed using SeaDAS 7.1 software.

More than 450 MODIS Aqua and Terra satellite products, recorded in 2013 and 2014, were used. They cover periods with both high and low Danube water levels. In Fig. 2, the yellow-red dots (266) represent days when data coming from both platforms were identified to be cloud free for our AOI. This was done by visual inspection. The dark blue dots are days when Aqua-Terra pairs do not meet the above mentioned quality control condition and can fall into one of the following category: only the image from one platform is cloud free, Aqua product is cloud free and Terra product is partially covered by clouds (and vice versa), or both products (from the two satellites) are heavily affected by cloud cover. The first category products (yellow-red dots) were used for all the following analysis, except for computing the monthly products, were second category datasets (dark blue dots) were also used in order to maximize the number of available bins (cells/pixels) used to derive the composite products.

Accurate remote sensing reflectance values ( $R_{rs}$ ,  $sr^{-1}$ ) can be obtained only if proper processing is applied to Level 1 datasets. Removing the atmosphere contribution to the total radiation that reaches the sensor is probably the most important step. Atmospheric corrections usually used in oceanographic applications are

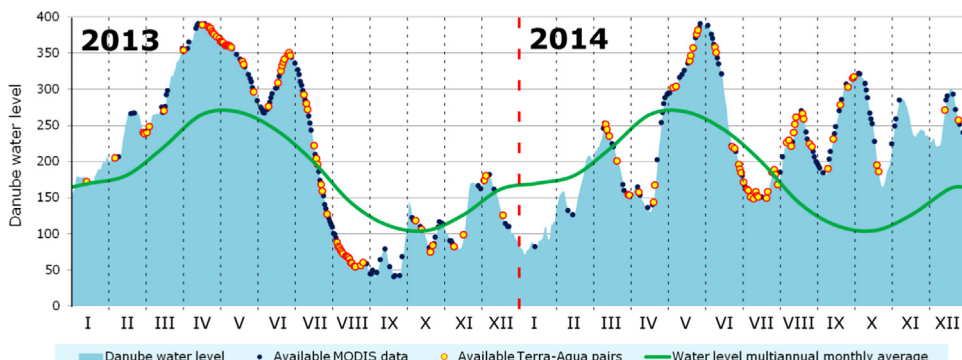


**Fig. 2.** Hydrological regime of Danube river during 2013–2014 time period (data source: River Administration of the Lower Danube) and corresponding days with cloud-free MODIS data. The green line represents the water level multiannual (1941–2011) monthly average, the dark blue dots are days when MODIS semi cloud-free products are available and the yellow-red dots are days when MODIS cloud-free Terra-Aqua pairs are available. (For interpretation of the references to color in this figure legend, the reader is referred to the web version of this article.)

based on the assumption of zero or very low reflectance values in the NIR part of the electromagnetic spectrum. These algorithms tend to fail in coastal waters (so called Case 2 waters, as defined by Morel and Prieur, 1977), since the high suspended matter concentrations lead to significant values of water leaving reflectance in the NIR bands. It is therefore necessary to use adapted methodologies in order to correctly process remote sensing data in coastal areas and remove the influence that aerosols have on top of the atmosphere measured radiance. This influence can be significant, since at the altitude of a satellite sensor, more than 80% of the light reaching the detector may have an atmospheric origin (Morel, 1980).

For the purpose of the present study three atmospheric correction algorithms were evaluated. Two of them are specifically designed to yield good results in coastal areas (Goyens et al., 2013), while the third one was not even developed for water applications, but for land. The reason for analyzing this third alternative is that it provides operational MOD09 products, already corrected for atmospheric effects. These have been successfully used for turbidity and TSM analysis in the Gironde estuary (e.g., Doxaran et al., 2009).

The first algorithm considered is the MUMM methodology (Ruddick et al., 2000), which is basically an extension of the standard algorithm used in Case 1 waters (Gordon and Wang, 1994). Assumption that water-leaving radiance in the NIR is zero is replaced by the assumption of homogeneity of the ratio of the both aerosols reflectances and water-leaving reflectances at 765 and 865 nm over the entire analyzed area. The algorithm was developed and tested using data collected in the North Sea, i.e. in moderately to highly turbid waters. It is also based on the NIR similarity spectrum developed by Ruddick et al. (2006), which is valid in the case off moderately turbid waters but fails in highly turbid ones (Doron et al., 2011).

The second methodology taken into consideration is the NIR/SWIR switching algorithm proposed by Wang and Shi (2007). This algorithm was designed in order to yield good results in different environments, from clear waters up to extremely turbid ones where the seawater reflectance remains negligible in the SWIR domain, independent of the load of suspended particles (Knaeps et al., 2012). The algorithm is based on first identifying the high and low turbidity areas by calculating a Turbidity Index (Shi and Wang, 2007), hereafter called Shi Turbidity Index. Based on a threshold of 1.3 of this index, the areas are divided into low and high turbidity zones. This value, of 1.3, is the one considered to be the most appropriate one for general classification of low-high turbidity areas (Wang and Shi, 2007) and is the default implementation in SeaDAS processing modules. For the first category the standard NIR atmospheric correction procedure is used, while for high turbidity areas the SWIR band replaces the NIR one. The switch between NIR and SWIR bands is dictated by computation of the Shi Turbidity Index, using bands  $\lambda=748$  nm,  $\lambda=1240$  nm and  $\lambda=2130$  nm, by applying the formula:

$$T_{ind}(748, 1240) = \frac{\Delta\rho^{(RC)}(748)}{\Delta\rho^{(RC)}(1240)} \exp\left\{-\frac{492}{890} \ln\left(\frac{\Delta\rho^{(RC)}(1240)}{\Delta\rho^{(RC)}(2130)}\right)\right\} \quad (1)$$

where  $\Delta\rho^{(RC)}(\lambda)$  is the Rayleigh-corrected (RC) top-of-atmosphere (TOA) reflectance at a given wavelength.

Using only SWIR based correction, in areas where turbidity values are low, the algorithm might yield worse results than the standard one. The main cause is that SWIR band signal-to-noise ratio (SNR) is low and not adapted to ocean colour applications. Therefore, combining the two methods assures a more accurate ocean colour data processing at each pixel level (Wang and Shi, 2007).

Last, we have evaluated the results of the standard processor for atmospheric correction used for retrieving operational

products MOD09 (Vermote and Kotchenova, 2008), distributed by NASA. The algorithm is assuming for a Lambertian surface, therefore it is not accounting for surface directional effects. The resulting products are the dimensionless surface reflectance values (R). These products were designed for land applications and clouds detection, therefore it uses methods and spectral bands for atmospheric correction that are not suited for ocean colour applications, since in such cases the radiometric accuracy should be greater. Nonetheless, MOD09 products have been successfully used in coastal turbidity and TSM analysis by many authors up to this moment, since the high concentrations of suspended matter in these areas do not require such finer sensitivity as for Case 1 waters. Doxaran et al. (2009) used MO09GQ data to analyze TSM dynamics in the Gironde estuary, Miller and McKee (2004) used another version of the same product (MOD02QKM, in conjunction with MOD03) to analyze the distribution of TSM in several coastal areas in the Gulf of Mexico. MYD09 data was also the main source of information for monitoring spatio-temporal variability of turbidity and TSM in the Adour river plume (Bay of Biscay) (Petus et al., 2010 and 2014).

### 2.3. Establishing the relationship between in-situ measurements and red-NIR bands

Many algorithms focused on establishing a relationship between water leaving reflectance and Total Suspended Matter (TSM) and few on retrieving turbidity (Dogliotti et al., 2015). This has the disadvantage that TSM retrieving algorithms are more sensitive to multiple factors, such as particle density and refractive index, while turbidity retrieval algorithms are less sensitive than more robust. This is due to the fact that turbidity is an optical property, thus more correlated to reflectance through back-scattering coefficients (Dogliotti et al., 2015). Nevertheless, for the Danube Delta coastal area it is still an increasing need for establishing a robust relationship between turbidity and TSM. Dogliotti et al. (2015) proposes a combined methodology for turbidity retrieval, based on Nechad et al. (2009) general algorithm, using a switch computation between  $\lambda=645$  nm and  $\lambda=859$  nm band, depending of the values of  $\rho_w$  (water leaving reflectance), which is defined as:

$$\rho_w(\lambda) = \pi L_w(\lambda)/E_d^{0+}(\lambda) \quad (2)$$

where  $L_w$  is the water-leaving radiance ( $\text{W m}^{-2} \text{sr}^{-1} \text{nm}^{-1}$ ) and  $E_d^{0+}$  ( $\text{W m}^{-2} \text{nm}^{-1}$ ) is the above-water downwelling irradiance.

The later one (NIR band, 859 nm) can be used to generate maps of turbidity in moderate to highly turbid waters, while the red band, more sensitive, is used for lower turbidity values. The range of values for which the methodology was tested is between 0.5 and more than 1000 FNU (such as in the Gironde estuary).

In order to establish a relationship between turbidity (in-situ measurements) and  $R_{rs}$  in red and/or NIR spectral bands, a first required step was to determine the best suited atmospheric correction algorithm. After such methodology was chosen, the entire set of remote sensing data was processed. Products corresponding to the field campaigns days, when in-situ T values were obtained, were selected and for each field measurement point the remote sensing reflectance ( $R_{rs}$ ) value was retrieved. Taking into consideration the hour when in-situ measurements were made, according to Table 1, the match-ups were made using MODIS-Aqua or Terra derived  $R_{rs}$ . For the scope of this paper,  $R_{rs}$  is defined as:

$$R_{rs}(\lambda) = nL_w(\lambda)/F_0(\lambda) \quad (3)$$

where  $\lambda$  is the wavelength,  $nL_w$  is the normalized water leaving radiance and  $F_0$  is the mean solar irradiance, just above the water surface.

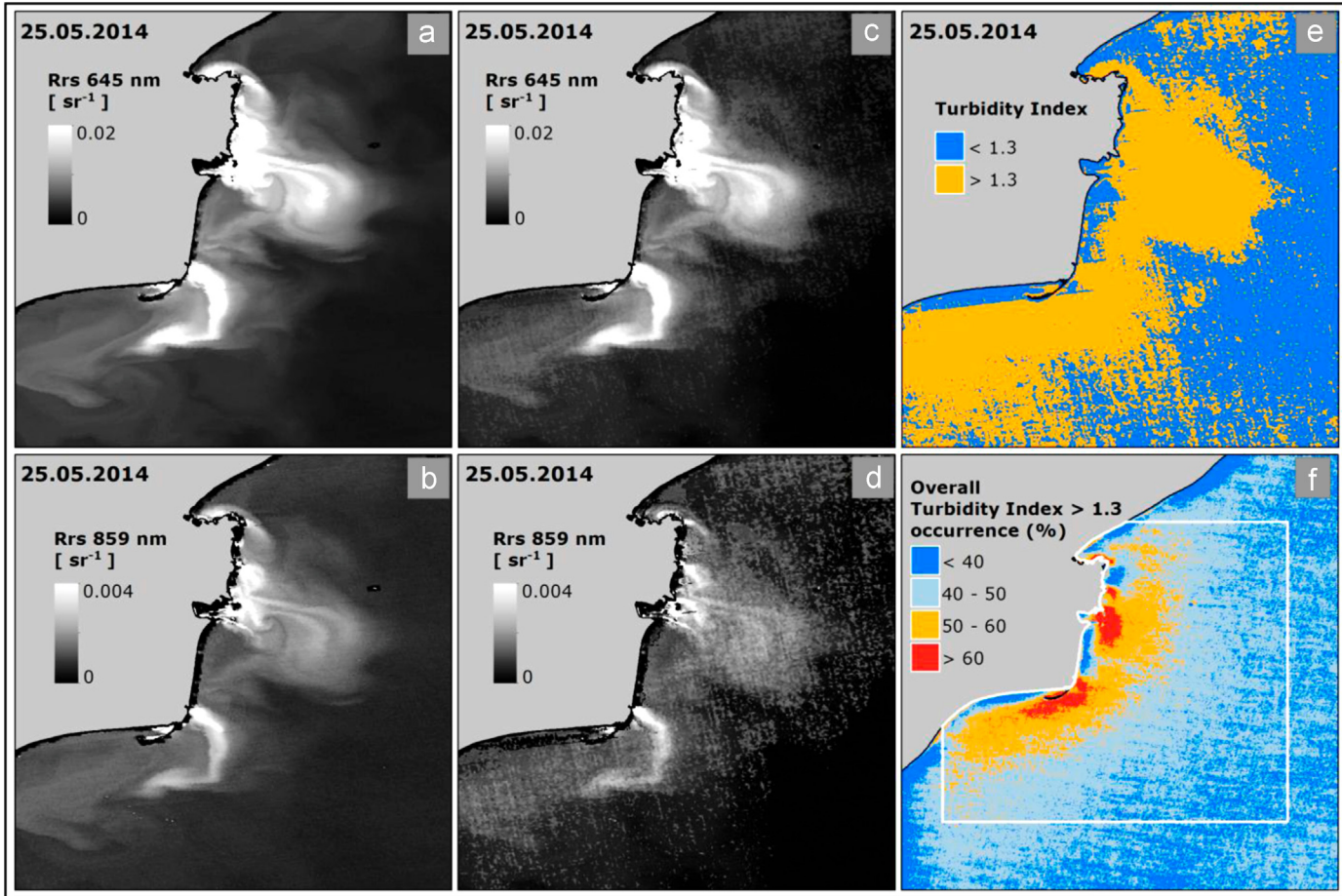


**Fig. 3.** Comparison between two atmospheric correction algorithms: MUMM (a and b, for two distinct spectral bands) and NIR/SWIR switching method (c and d); Shi turbidity index for the same image is presented (e) and also the overall Shi turbidity index larger than 1.3 occurrence (in percentages) is shown (computed for two years period, using more than 260 MODIS products).

Based on these match-ups, an empirical relationship was derived between  $T$  (FTU) and  $R_{rs}$  ( $\text{sr}^{-1}$ ).

#### 2.4. Turbidity maps generation

Using the corrected Level 2 MODIS product computed using SeaDAS software, with all the masks that might cause bad pixel values (such as the common stray light flag found near the coastline), the equation determined in the previous step was used to calculate the turbidity values at each pixel. For analysis concerning the variations of turbidity from one day to another, Aqua and Terra products were averaged for each day. In order to produce monthly composite products, all available information coming from both Aqua and Terra platforms for each month was also averaged. In order to keep track of the quality of the monthly products, the number of bins (cells) used to compute each final cell value was registered. We can therefore make use of such data knowing the amount of information than was put into its derivation.

### 3. Results and discussion

#### 3.1. Regional algorithm for $T$ retrieval using MODIS datasets

##### 3.1.1. Atmospheric correction of satellite data

Since atmospheric correction procedure is of uttermost importance for accurate turbidity estimations using remote sensing data,

capabilities of different algorithms were tested. Even though it was expected not to yield good results, the standard correction algorithm (Gordon and Wang, 1994) was applied and indeed failed in some areas close to the river mouth, where turbidity values are higher and therefore NIR signal is not close to zero. Further, we continued with evaluating the previously mentioned atmospheric correction algorithms.

**3.1.1.1. MUMM and NIR/SWIR switching algorithms.** Multiple satellite products were processed using both atmospheric correction algorithms and the results were qualitatively evaluated in order to select the most appropriate one. The selection was based on visual comparisons of the results and, thereafter, analysis of pixel values for specific areas in order to evaluate the differences between the two algorithms and the quality of each.

Significant differences were expected to be identified between the two methods in the proximity of the river mouths, where turbidity values are higher and therefore the NIR/SWIR algorithm would perform better, but such differences were not observed in the moderately turbid waters of our AOI. The MUMM algorithm performed well for both red ( $\lambda=645 \text{ nm}$ ) and NIR ( $\lambda=859 \text{ nm}$ ) band (Fig. 3(a) and (b)). Just by visual inspection, the NIR/SWIR algorithm results were less satisfactory, most probably due to low SNR of the SWIR bands. This low SNR also probably results in some artefacts visible in Fig. 3(c) and mainly in (d), in the NIR band.

The default value for  $T_{ind}$ , which dictates the usage of SWIR band, is 1.3 (Wang and Shi, 2007). This means that if the  $T_{ind}$  is greater than 1.3, the algorithm switches from using the NIR bands to the SWIR ones. Modifying this threshold might improve the

quality of the final products for specific areas, but this still does not account for low SNR of the SWIR bands. For the product in Fig. 3 (c) and (d) we have computed the corresponding  $T_{ind}$  (e). In areas closer to the shoreline (in orange), where turbidity values are expected to be higher, the  $T_{ind}$  imposes that NIR based method should be discarded. Very close to the coast however, the  $T_{ind}$  fails (probably because of the saturation at band 748 nm), for this specific case, to account for high turbidity areas. Using two years of MODIS data we have mapped the occurrence of  $T_{ind}$  larger than 1.3 (Fig. 3(f)) in order to better understand how often the SWIR bands should be used over a long time series of satellite products. This result gives us also a first glimpse of the turbidity dynamics, with areas closer to the river mouths being the most affected (red areas,

where SWIR bands should be used more than 60% of the time for atmospheric correction). Again, there are portions, very close to the shoreline, which appear to be low turbid waters. In fact, these results are due to the fact that, in such areas, satellite data is heavily affected by stray light. This effect is more obvious in the NIR bands and when using the NIR/SWIR algorithm, compared to MUMM. It is normal that NIR band is more affected by stray light, since the largest impact is to low radiance ocean observations that are within a few kilometres of bright sources such as clouds, coastlines, or sun glitter ([oceancolor.gsfc.nasa.gov](http://oceancolor.gsfc.nasa.gov)). When using the NIR/SWIR algorithm, a larger amplitude in  $R_{rs}$  can be observed between coastal and offshore areas compared to MUMM results, although the transition between the two is not visible.

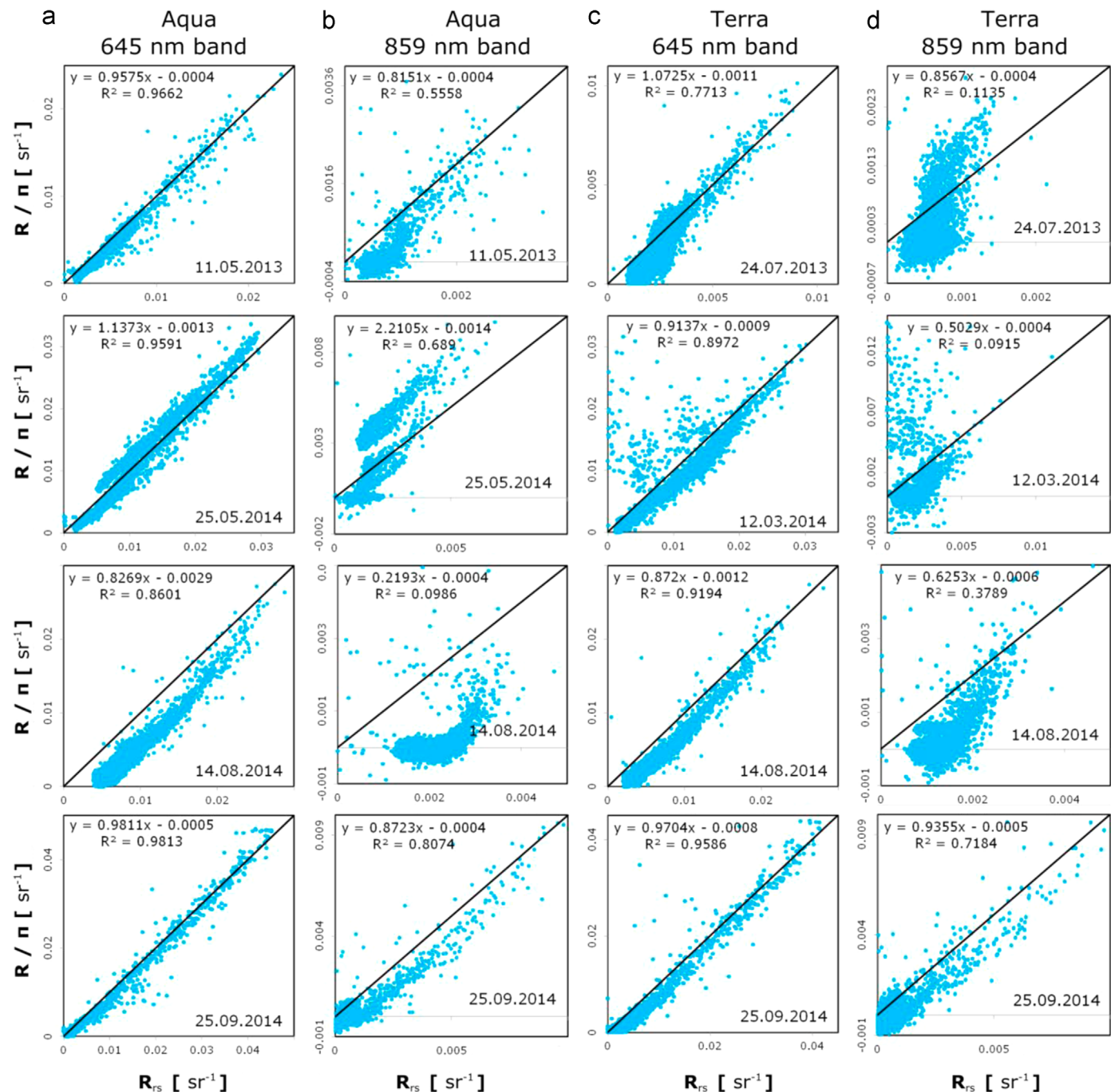


**Fig. 4.** Comparison between MUMM derived remote sensing reflectance ( $R_{rs}$ ) and MOD09 surface reflectance values ( $R = \pi * R_{rs}$ ) for different MODIS products. The first column (a) shows Aqua derived information from band 645 nm. Column (b) is based on data derived from same Aqua products, but for band 859 nm. Columns (c) and (d) reflect the same information for Terra sensor.

Based on the criteria mentioned above, the decision was to use MUMM algorithm for all further processing. This is sustained also by the fact that the AOI is characterized by medium turbidity values, as we shall see further. Therefore, it is expected that the NIR bands approach should not yield good results and the switching to SWIR based atmospheric correction should not be necessary.

**3.1.1.2. MUMM and MOD09 processor for atmospheric correction.** We have used MOD09GQ (Terra) and MYD09GQ (Aqua) surface reflectance products, which are daily Level 2 gridded (L2G) products comprising the first two spectral bands of MODIS (red and NIR) at 250 m spatial resolution. Since it reflects the same characteristics in terms of spectral and radiometric quality as the other products from the MOD09 family, we shall further refer to it as generically MOD09.

In order to better assess the similarities and differences between MUMM processed datasets and MOD09 surface reflectance products, we have analyzed scatter plots between these two products for several days (Fig. 4). The first observation made is the poor correlation between the two products in NIR band as compared to the red one. This is simply due to the lower water-leaving signal in the NIR, resulting from high light absorption by pure water in this part of the spectrum. Even in cases where the correlation in the red band is very good (on 25.09.2014), there are still large differences to be noticed in the NIR one. As a result of different aerosol optical thickness estimation techniques and also because the MOD09 algorithm does not take into consideration the directional effects of the water-leaving signal (computations are performed under the assumption of a Lambertian target), the

slope of the relation between the two set of values is not always close to 1. The same pattern is generally maintained between Aqua and Terra for the same day of acquisition, both in the red and in the NIR bands. Other differences between the two products refer to the fact that clouds are not masked out in the MOD09 product, but this is a minor issue since a cloud mask can be extracted from the product and applied after on the reflectance layer.

Visual assessment of the quality of the two products (Fig. 5) reveals, as could be expected, that: MOD09 surface reflectance values are not properly computed in coastal areas, and this is more obvious in the NIR band. Even for products that obviously are of good quality (c), the MUMM alternative (e) is still better, lacking some artefacts that appear in MOD09 (such as the one south of Sfântu Gheorghe River mouth). The positive thing about MOD09 is that fewer pixels appear to suffer from stray light effects.

Although MOD09 has proved useful in highly turbid waters by many studies, as mentioned previously, for our AOI more accurate atmospheric correction procedures are required. In conclusion, we do not advise the use of MOD09 products in the Danube Delta coastal area for good quality ocean colour processing, but since it represents a very handy resource of data, it might be useful for studies that do not require absolute turbidity (or any other variable) values determination. For example, it might be of great service for studies analyzing trends over long time series of data. These recommendations refer only to the red band ( $\lambda=645$  nm), since the NIR band ( $\lambda=859$  nm) clearly has important flaws. In any case, usage of MOD09 products should be treated with care and its drawbacks when applied to water studies should always be accounted for.

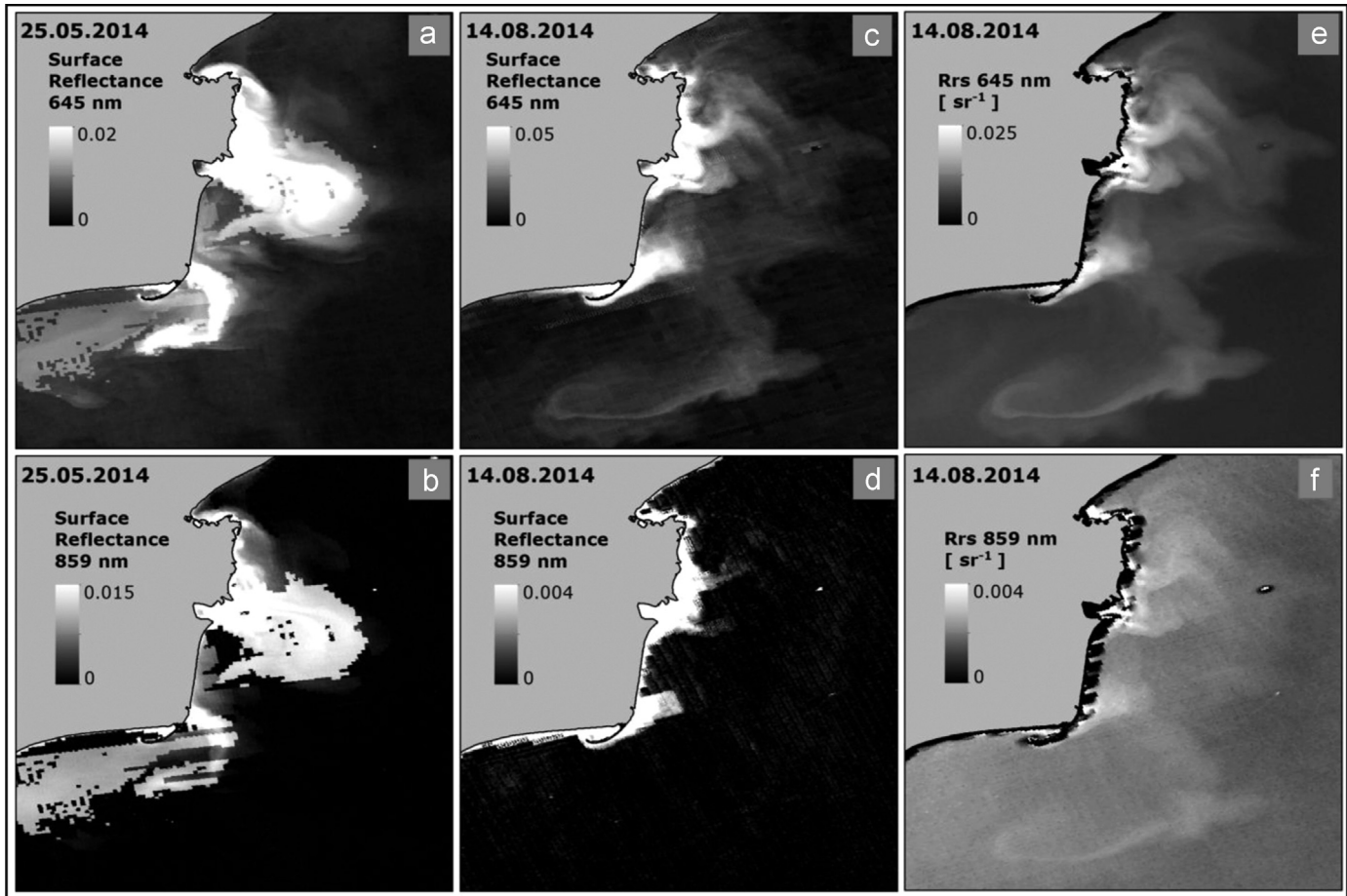


**Fig. 5.** Comparison between two atmospheric correction algorithms: default methodology for MOD09 products (a)–(d), expressed as ( $R=\pi * R_{rs}$ ) and MUMM algorithm (e) and (f), expressed as  $R_{rs}$ ; examples are shown for both 645 and 859 nm bands.

### 3.1.2. Regional relationship between in-situ measurements (turbidity) and satellite-derived remote sensing reflectance in red and NIR bands

The relationship between turbidity (in-situ measurements) and MODIS-derived  $R_{rs}$  values follows an exponential curve in the red band (Fig. 6a). In the NIR, the relationship is linear, avoiding in this way the saturation that occurs in the red band starting at approximately 40 FTU. The overall distribution of match-ups follows the same pattern already discussed in other studies (Doxaran et al., 2006; Nechad et al., 2010), where typical  $R_{rs}$  signal increases with increasing concentrations of particulate matter and turbidity. This occurs first in visible part of the electromagnetic spectrum, then in the red and finally in the near-infrared. Generally, there is a good agreement between the relationships presented in Fig. 6 and studies addressing the same problem over other areas (Dogliotti et al., 2015). The same saturation of the red band occurs starting at similar turbidity values, while  $R_{rs}$  in the NIR band does not saturate in this range of turbidity values (< 160 FTU).

The NIR band can be used for high turbidity values (> 50 FTU), but these values do not occur often in our AOI. This statement is based on a previous study that showed medium turbidity values in the Danube coastal area (Güttler et al., 2013), and is supported by the comparison between our sets of measurements and those reported by Dogliotti et al. (2015). In this latter study, thresholds for water reflectance  $\rho_w(645)$  (not compensated for directional effects) of 0.05 and 0.07 are proposed to determine the switch between using  $\rho_w$  in the red or the NIR band to compute turbidity (up to 0.05, the red band is used, after 0.07 the NIR, and between 0.05 and 0.07 the two algorithms are blended). In our AOI, after evaluating 266 images recorded in 2013 and 2014, we have observed that 3.44% pixels fall in the 0.05–0.07 range and only 1.05% of pixels have  $\rho_w(645)$  values larger than 0.07 (Fig. 7). This means that only in 1% of the whole area the NIR band should be used (this limit is also shown in Fig. 6 with a dotted red line; in-situ measurements that go beyond this line can be considered as exceptional cases). This analysis was performed only for a limited area close to the river mouths (using a 30 km radius from each river mouth), where turbidity values are high, and therefore  $R_{rs}(645)$  should also have the highest values. If the analysis is extended to the entire study area, the percentages would be much lower. We can therefore conclude that the AOI is characterized by moderately turbid waters and the relationship established between turbidity and  $R_{rs}(645)$  is to be used with confidence for computing specific products and for analyzing the dynamics of the turbidity spatial extension.

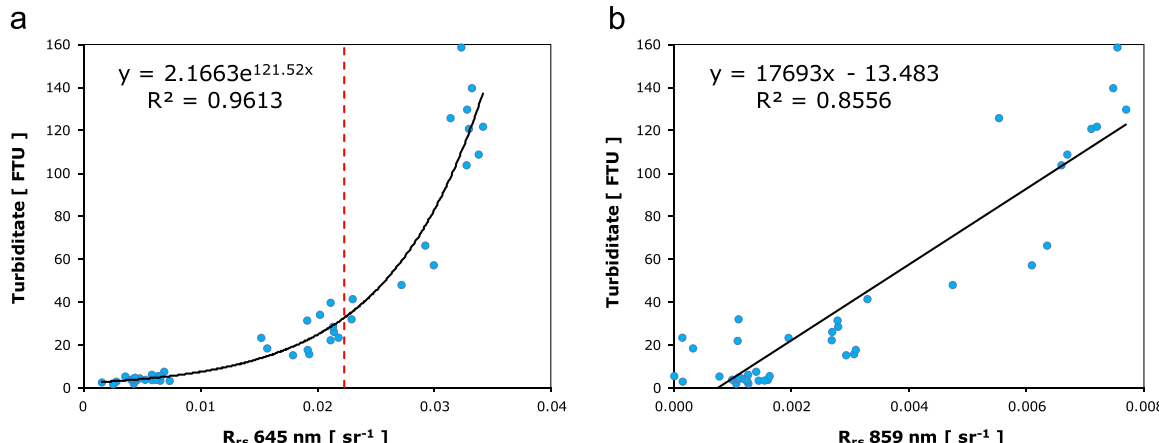


**Fig. 6.** Relationship between turbidity in-situ measurements and MODIS derived  $R_{rs}$  in the 645 nm spectral band (a) and 859 nm band (b); the red dotted line in (a) represents the limit after which the probability of cases is around 1%. (For interpretation of the references to color in this figure legend, the reader is referred to the web version of this article.).

### 3.2. Spatio-temporal dynamics of water turbidity

#### 3.2.1. Hourly dynamics

Due to the fact that MODIS sensors are mounted both on Aqua and Terra platforms, it gives us the possibility to analyze the dynamics of turbidity within the two daily successive overpasses, i.e. within a period in between one hour and a half and four hours, depending on the satellite orbits each day. Multiple scatter plots show comparison of the water turbidity mapped using Aqua and Terra satellite data recorded on a same day (Fig. 8). These comparisons were made on days representative of different wind conditions. It was indeed a challenge to find quality satellite products for days when the main direction of the wind was from East side, since these meteorological conditions are not to be often found in our AOI.

Analyzing the scatter plots, points under 1:1 line represent an increase in  $T$  between Terra and Aqua overpasses. The points are closer to this line (more grouped) for lower values than for high ones. This reflects a perfectly normal behaviour since moderately to highly turbid areas, like ones close to the river mouths, are more dynamic and more prone to change in a two hour interval. Therefore, most of the graphics present a “normal” distribution of points, with a scatter getting higher as  $T$  values increase. Higher wind speeds usually correspond to higher scatter in the relationship, but this is not always the case, meaning that other factors on top of wind, such as marine currents, contribute to the dynamics of the river plume. Another parameter to be analyzed is the slope of the linear equation fitted between the two sets of values: this slope is generally lower than 1. This might indicate variations of water turbidity between Aqua and Terra overpasses, but more likely it indicates also differences in radiometric accuracy between the two sensors. This is sustained also by the argument that there is a great correlation between the two datasets, with high determination coefficients. Other studies have showed that both sensors (Aqua and Terra) are affected by aging factors (Franz et al., 2008). Nonetheless, Terra is more prone to such sensor deterioration, meaning the amount of captured energy is decreasing over the years, with the radiometric response degrading more in the lower wavelengths domain (Franz et al., 2008). The same trend is to be observed also in the longer wavelengths, but with minor differences, which is the case of the present study, where the red band is used. Our results are in very good agreement with such observations, the slope of the equation between the two sensors indicating a slightly overall lower reflectance values registered for Terra, compared to Aqua products. Since the disparities are small in magnitude, differentiating between the two aspects causing this

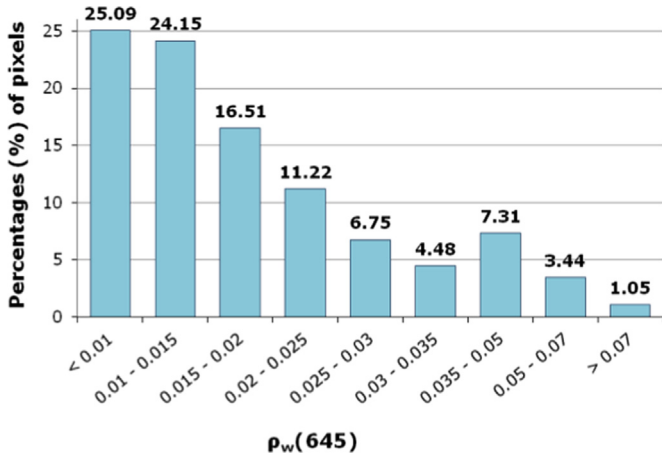


Fig. 7. Overall distribution of reflectance values for 645 nm band ( $\rho_w = \pi * R_{rs}$ ), in the Romanian coastal areas, computed for two years period (2013–2014) using more than 260 MODIS products.

problem (dynamics of turbidity or radiometric accuracy) would be a very difficult task, outside the scope of the present study. Other important differences between the two sensors include the more visible stripping effects in Terra products. The limitations of Terra for ocean colour application are well known (Franz et al., 2008), but for the present study we consider them not to be of primary importance since they are not significantly affecting the results of the analysis, the radiometric uncertainties between Aqua and

Terra being of higher importance for retrieval of other parameters, besides turbidity, using lower wavelengths bands, such as chlorophyll concentration.

The least dynamic situation between Aqua and Terra occur during periods with wind from the North, even with high speed values, which do not interfere with “normal” general conditions of the area (dominated by Northern winds and currents). These winds do not set up conditions for strong vertical mixing of the water column, therefore the magnitudes of resuspension might also be low. When analyzing the turbidity maps used to generate the scatter plots, it appears that the extension of the sediment plume is larger when southern winds blow, likely due to offshore Eckman transport.

### 3.2.2. Daily to weekly dynamics

Since there are no important variations between the two sensors passes, Aqua and Terra turbidity products were averaged to generate daily products used to analyze the river plume dynamics over multiple days periods. For this specific purpose we have selected three time periods corresponding to different hydrological conditions: 22 April to 11 May (Fig. 9a) and 5–26 August 2013 (Fig. 9b) respectively corresponding to high and low Danube discharge values and 23 June to 27 August 2014 (Fig. 9-c) for moderate water levels. Water level is depicted using a blue line in Fig. 9. The red line represents the evolution during the already mentioned periods of the average turbidity value in the AOI, while the green line corresponds to a smaller area within a 30 km buffer from the river mouths. The two areas are reflecting the same

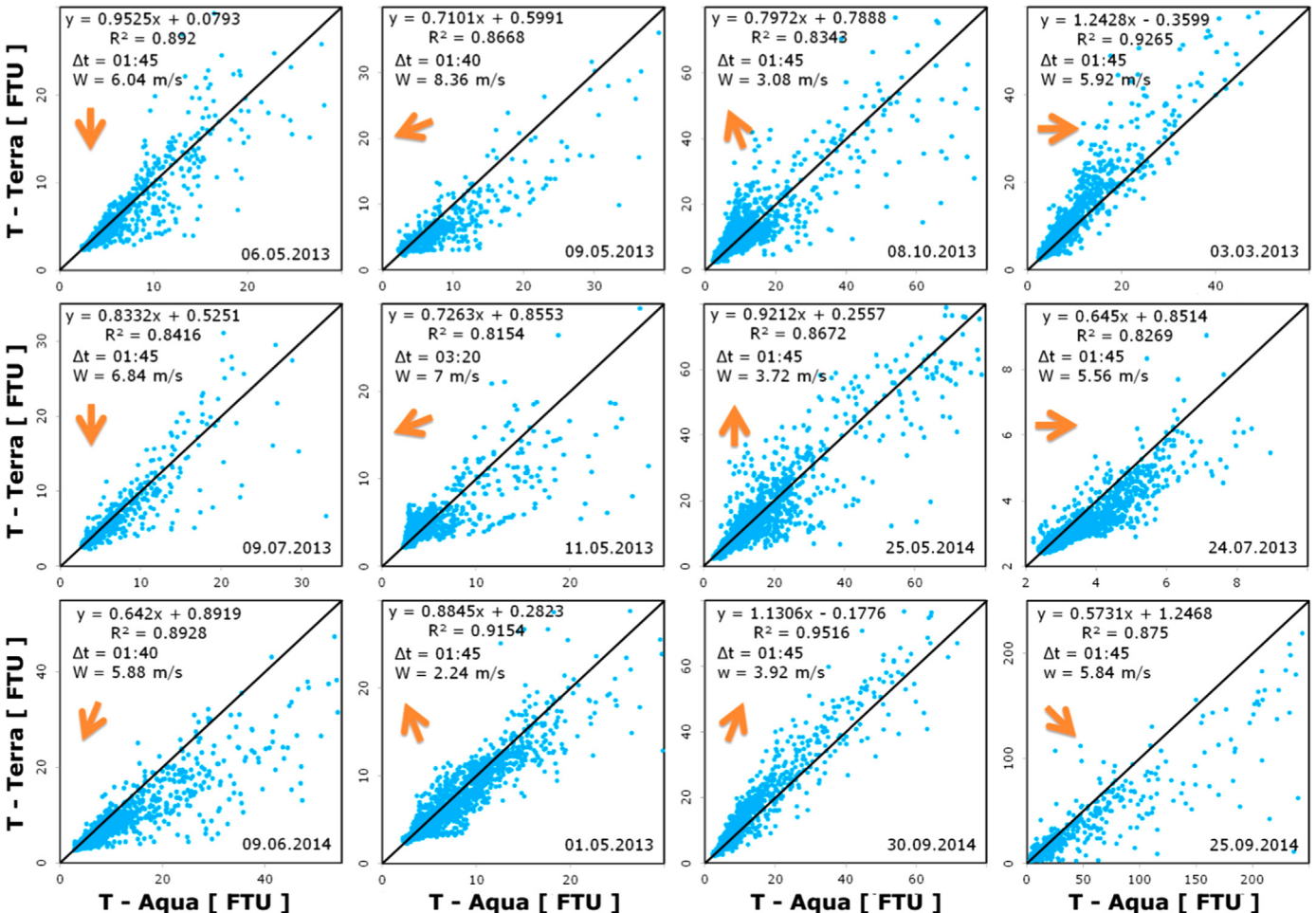
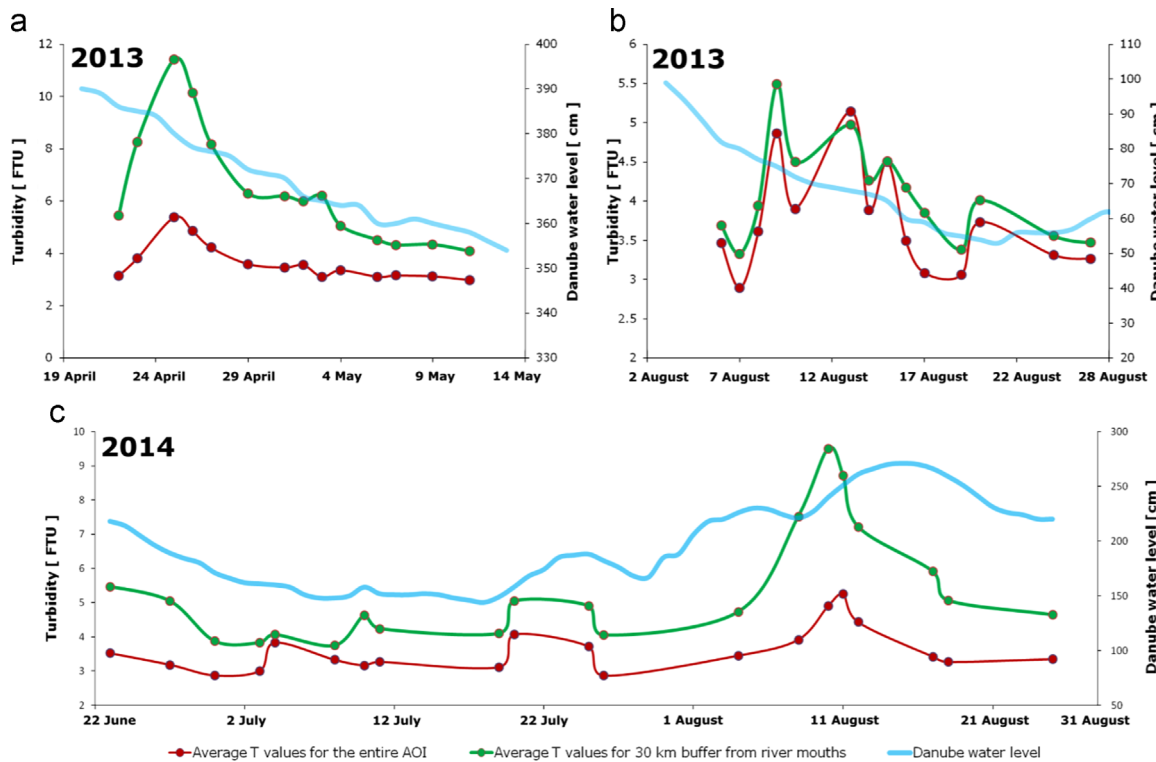


Fig. 8. Scatter plots of Aqua and Terra derived  $R_{rs}$  values for 645 nm band, where  $\Delta t$  is the time difference between the two satellite passes (in hours and minutes),  $w$  is the mean wind speed calculated for 24 h before Aqua pass and the orange arrows represent the general wind direction for the same time period.



**Fig. 9.** Daily dynamics of turbidity (based on MODIS data) in the Romanian coastal waters; blue lines represent the Danube water level, green lines are the average turbidity values computed for a buffer area of 30 km from river mouths, and the red lines are average turbidity values for the entire AOI.

trends in T averages, obviously with a higher dynamic in the proximity of the coast. There are also inverse situations, when one value is getting higher while the other decreases (and vice versa), such as on 3 May 2013 or 10 July 2014. These examples reflect periods when sudden variations of turbidity occur near the river mouth but a time delay is necessary before these variations impact the entire AOI.

During the second time period (b), even if the dynamics might seem larger than for high discharge levels, the amplitude is much lower, 2.16 FTU compared with 7.34 FTU in case (a). For both situations, the general trend of Danube water levels is decreasing. Between the two parameters (water level and turbidity) a very good correlation is observed for all the analyzed time periods. The solid discharge (SD) values measured on the Danube River at the same hydrological station as for the water levels (Tulcea) were available only in 2013. The correlation between water turbidity daily averages and SD values is good, but lower than that observed between water turbidity and water level. This is due to the fact that the SD tends to have a much wider dynamics than the liquid discharge. In both cases, the relationship with T averages in the coastal area is more obvious when the water level or solid discharge values are higher.

The long time period in 2014 (c) shows a quite obvious correlation between all parameters, but what is most important here is the clear evidence of maximum turbidity values occurring just before the maximum for water level (middle of August). This behaviour was already documented for the river solid discharge (Vidrascu, 1921) and our observation shows that the same behaviour applies to coastal area turbidity values. This interval, of almost six days, between the two maxima is also influenced by the fact that water levels are measured at Tulcea hydrological station (approximately 80 km upstream Sulina River mouth) and the effects observed in the river take time before being reflected in the coastal area. Nevertheless, this period should be less than 1 day, even in low discharge conditions. It is therefore correct to

conclude that the gap between maximum turbidity values in the coastal area and maximum water levels on the Danube River is a consequence of the same gap between solid and liquid discharges on the river.

By analyzing all the details above regarding daily dynamics of the average value of turbidity in the Danube Delta coastal plain, one of the main conclusions to be drawn is that the river has a great influence on the turbidity changes that occur in the coastal area, close to the river mouth, but also further offshore.

### 3.2.3. Monthly (seasonal) dynamics

Monthly products for 2013 and 2014 (Figs. 10 and 11) were computed using all the available MODIS data for each month. In order to be able to draw correct conclusions based on these maps, each product was marked according to the amount of data used to produce it. In this sense, data marked with only one \* means that only five or fewer bins (cells) were available to be averaged for the creation of the final product, for the most part of the AOI (at least 75% from the total surface). Using the same logic, data marked with \*\* were produced using more than five, but up to 15 bins and, finally, maps that are rated with \*\*\* are the result of averaging more than 15 bins for at least 75% of the AOI surface. Based on this information, the last category is the most valuable one since it represents a synthesis of large quantity of data. Depending of the amount of data available for each monthly product, some artefacts are likely to appear when not enough information is at disposal. This is the case in January 2013, February, October and November 2014, when compilation (averaging) using few images, with different turbidity values, conducted to the appearance of areas with spatially abrupt variations in turbidity, especially offshore, where low values of turbidity would require a more sensitive band than the red one used in this study, besides spatial consistency. These products are to be used with care, since it might induce false conclusions. At the same time these datasets are not to be discarded, since closer to the river mouth the information they

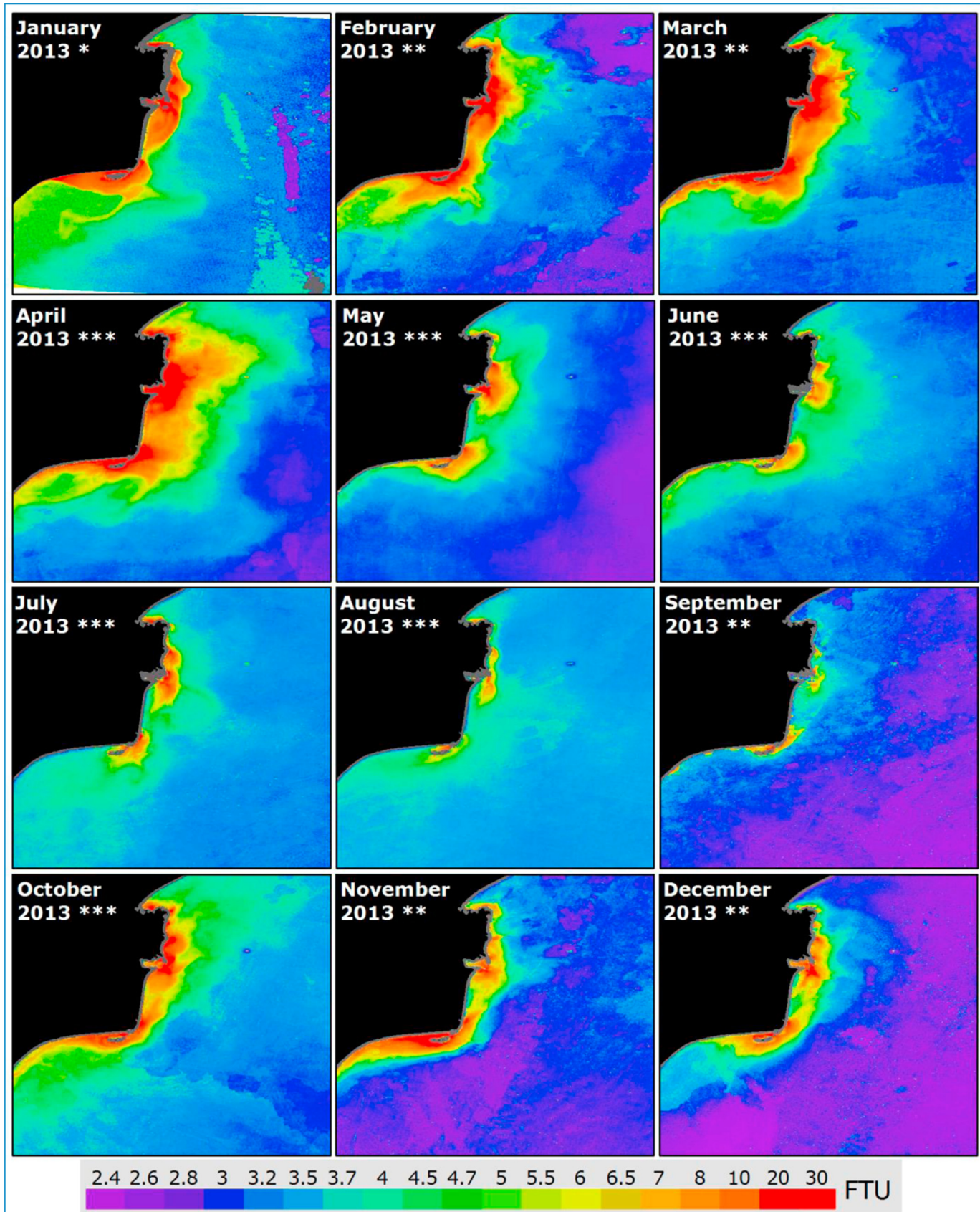
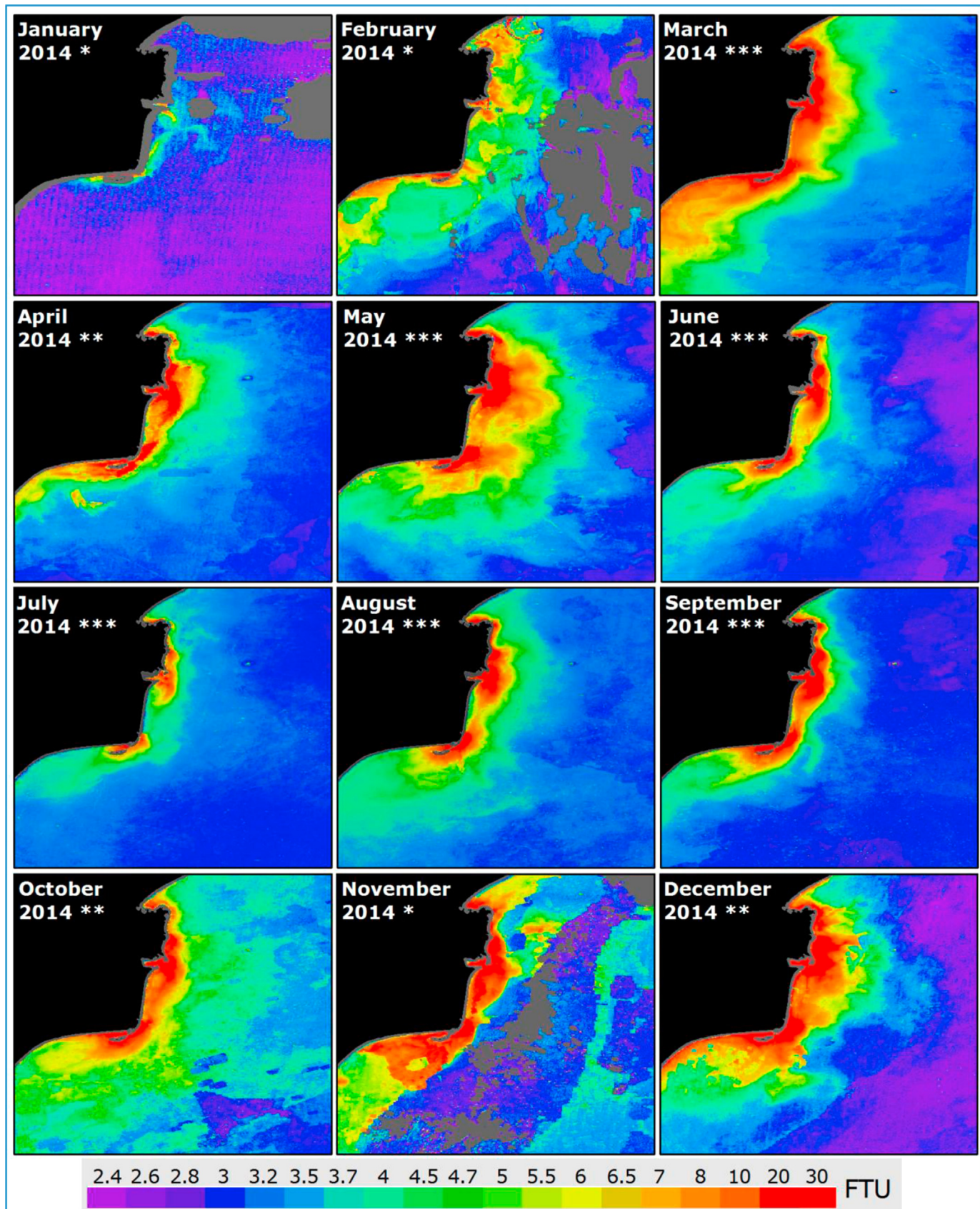
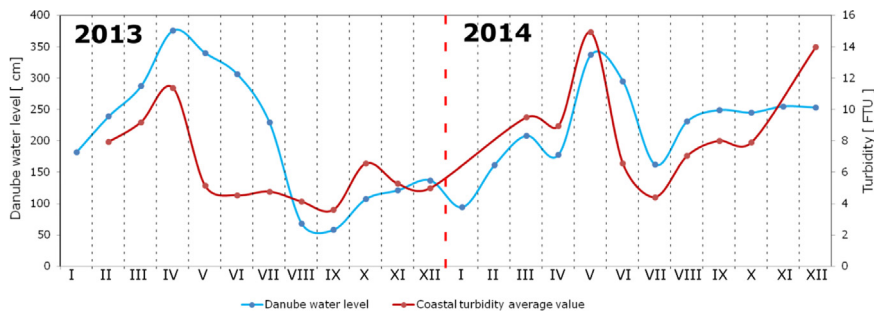


Fig. 10. Monthly averaged turbidity maps of the Romanian coastal area in 2013, based on MODIS data.



**Fig. 11.** Monthly averaged turbidity maps of the Romanian coastal area in 2014, based on MODIS data.



**Fig. 12.** Two year evolution of monthly mean turbidity values in Danube Delta coastal area (red line) in correlation with river water level values (blue line).

provide might be more useful and correct than in offshore areas (required sensitivity in accordance with turbidity ranges to be observed, meaning for retrieving higher turbidity values the involved uncertainties are lower than for low turbidity levels). Even months with high number of cloud-free products (monthly averages rated with \*\*\*) might be affected by such problems (e.g., in October 2013).

Regarding the monthly products and seasonal variability of turbidity observed in the coastal area, the close correlation between the hydrological regime of the Danube River and the magnitude of the river plume (great spatial extent and high turbidity values near the river mouths) must be highlighted. During spring high discharge values of the Danube, the extent of the river plume is maximum (April 2013 and May 2014). For these two months the turbidity values higher than 4 FTU can be found up to 75 km and 65 km, respectively, offshore in the East direction. Also, these time periods correspond to the highest overall average values of turbidity, with areas where turbidity is higher than 30 FTU covering large areas in front of river mouths. In contrast, months of low Danube discharge rates exhibit low turbidity values over all the coastal area and a limited extension of the turbid plume. In August 2013, values larger than 4 FTU are all found within 10 km from the river mouths in the Eastern direction. However, due to long-shore sediment transport by currents flowing North to South, the plume extends South 25 km from the Sulina mouth and 50 km from the Sfântu Gheorghe mouth. The same situation can be observed in July 2014, when turbidity is lower than 4 FTU in areas located more than 10 to 20 km away from the coast. The river plume reveals the same southern dispersion, along the shoreline. Further offshore, water clarity seems to be higher in this situation than in August 2013, probably due to lower phytoplankton concentrations in 2014. This hypothesis is sustained by the analysis of the standard Level 3 monthly Chlorophyll-a concentration product distributed by Ocean Biology Processing Group (OBPG) at NASA's Goddard Space Flight Center: algal development was stronger in 2014, but closer to the shoreline, while in 2013 the extension of the production zone extended further offshore. In any case, this requires further investigation, since standard algorithm for Chlorophyll-a concentration retrieval in this area might be associated with significant errors.

The turbidity regime in the coastal area is also influenced by other factors besides Danube discharge rates. Wind and marine currents can play a vital role in the dynamics of suspended sediments, but also the time of year can be of great significance. This can be observed during the studied years, 2013 and 2014, when analyzing months with almost similar water levels on the Danube: March and June, in 2013, and March and July, in 2014. During spring time, the extension of the turbid plume is evidently much larger than in summer, which means that the Danube solid discharge is getting lower, even if the liquid discharge remains almost the same.

During several time periods (e.g. April 2013 or March 2014), turbidity values are relatively high for large areas situated in the

South-West part of the AOI. This can be caused by sediments brought and trapped here by the long-shore currents from the North (Giosan et al., 1999), or by the resuspension processes that can increase in magnitude for this shallow water zone. Overall, from daily to seasonal regional perspective, this area is the second most turbid one after the ones situated right in front of river mouths.

The differences between the two years analyzed here are easy to see using the month of August as reference. The high Danube water levels in 2014 reflect very well in the river plume extension, compared to 2013. This good correlation between the two parameters can be observed also in Fig. 12. The graphic was constructed without using the information from turbidity products rated with only one \*. The trend exhibited by both parameters is the same in almost all the cases (except for some winter months), with a higher divergence between them for the time period May–July 2013.

### 3.3. Discussion

This study represents an important step forward in the understanding of turbidity dynamics and its consequences on the Danube Delta coastal area, by establishing a robust methodology for retrieving turbidity using satellite observations. Unlike other studies carried out before (Güttler et al., 2013), our methodology is based on local in-situ measurements, collected over a broad range of turbidity values, which assures a good characterization of the AOI. Also, atmospheric correction methods were evaluated specifically for the purpose of the study and considerations on MUMM algorithm suitability were made. Being the first attempt in using MODIS information for turbidity analysis in this region, it was possible to observe the spatial variations and amplitude of turbidity during the couple of hours between Terra and Aqua overpasses. Using MERIS derived information, the preferred datasets up to now for turbidity and TSM studies in the region (Güttler et al., 2013, Stanev and Kandilarov, 2012), such analyses are not possible, since the revisit time is lower (approximately every three days). We have shown that the hydrological regime of the Danube plays an important role in the coastal turbidity dynamics, but, as previously mentioned (Güttler et al., 2013), other factors also significantly influence the turbidity. We were able to indicate clear examples where, at monthly and seasonal scales, the time of year plays an important role in turbidity dynamics.

All these observations could be performed at small time periods (over one or two weeks), using daily products, and also seasonal, since monthly water turbidity maps were available. These monthly products are of great importance, because they can synthesize, for the first time, the information on how turbidity is changing in the coastal area of the Danube Delta over large periods of time.

#### 4. Conclusions

MODIS satellite data onboard Aqua and Terra satellite platforms continues to be a very valuable source of information for coastal applications, notably due to their high spatial resolution (250 m). For the Danube Delta coastal area it allows retrieval and mapping of turbidity values for large areas at once and, during cloud-free days, the dynamics of turbidity can be analyzed even within a couple of hours interval. Different types of MODIS products can be used for such studies, but it is highly recommended that ocean colour dedicated processors to be employed in such initiatives. Ocean colour algorithms provide adapted atmospheric correction, which is not really the case for land products. Only this guarantees a reliable estimation of water leaving reflectance that can be used further for direct inversion into water quality parameters, such as turbidity. Land products, such as the MOD09 Surface Reflectance, that were not designed for ocean colour applications, might be used for certain analysis, preferably in highly turbid waters, but the quality of the derived products has to be properly accounted for.

Atmospheric correction procedures constitute a key part of satellite data processing in the case of optically complex waters. For the Danube Delta coastal area, the MUMM algorithm proved to be the best suited solution for processing MODIS data. One of the main reasons is that the AOI is characterized by moderately turbid waters where the MUMM algorithm main assumptions are valid and so only the red band is required for turbidity retrieval. The NIR band would have proven useful only for highly turbid areas, where the seawater reflectance signal in the red band can become saturated, but it was not used in the present study.

The spatial extension of the river plume exhibits a typical behaviour, with values of turbidity decreasing as the distance from the river mouths increases. This was expected, as suspended solids progressively settle along the water column due to flocculation processes enhanced by salinity and as the speed of the water mass is decreasing. Coarse particles (flocs or aggregates) rapidly settle on the seafloor close to the coastline while fine particles are transported further offshore before they also settle and deposit. Close to the river mouths the turbidity estimations are mainly influenced by river solid discharge and resuspension processes, therefore by inorganic particles. Further away offshore, where turbidity values are much lower, phytoplankton (mainly organic) particles start playing a more important role. With regard to the dynamics of turbidity, our results showed quite limited variations within a few hours, i.e. from one satellite pass to another (Aqua and Terra). Similar limited variations were usually observed from one day to another. In the last case, turbidity distribution changes significantly only when high Danube discharge values are registered (sediment input from the river being also high). We can therefore conclude that the turbid plume in the deltaic coastal area is a system highly sensitive and controlled mainly by the changes in solid and liquid discharge rates of the Danube River. Nonetheless, we observed an increase in turbidity, regardless of Danube hydrological conditions, in the South-Western part of the AOI, where the shallow waters might induce high resuspension rates, especially during winter when the frequency of storms is higher and the long-shore sediment transport (LST) has the largest impact (50% of the total yearly LST occurs during December and January-Vespremeanu, 2007; Giosan et al., 1999). Therefore, it would be fair to say that the river has a great influence on turbidity plume extension and dynamics in the Eastern direction (offshore of river mouths), but close to the shoreline, other processes can have similar importance, such as waves and marine currents. This hypothesis needs, however, to be confirmed by analyzing a larger time series of data.

Based on the current study, important features of the AOI are to be confirmed by the extension and magnitude of turbidity values,

An interesting case was observed for the high erosive sector between Sulina and Sfântu Gheorghe, corresponding to low turbidity values, which means that there is a poor particulate matter input in this area (one of the main causes for high erosive rates). This is more evident during summer periods, when the turbidity lobes have a minor spatial extension, only in front of river mouths.

MODIS satellite data has the capability to reveal new insights on the extension and dynamics of river induced turbid plumes in the Danube Delta coastal area. Automated processing based on the methodology described in this study can be used to map water quality parameters for long time periods, since more than fourteen years of archive data is already available. Improvements of the current study are also foreseen, either by perfecting the relationship established between the remote sensing reflectance and turbidity parameters by using more in-situ observations, or by increasing the amount of satellite data and the analyzed time period. Also, it is envisioned that other parameters shall be included for a better understanding of turbidity dynamics, such as measurements of coastal currents, precise bathymetry or wave observations. The use of higher spatial resolution remote sensing data (e.g. Landsat) is also foreseen, since it can contribute significantly to understand local processes that affect specific focal points, such as Musura Bay (Sulina mouth) or Sacalin area (Sfântu Gheorghe mouth). Other in-water constituents must also be considered as highly important parameters for environmental analysis. Therefore, developing and calibrating a regional chlorophyll-a concentration algorithm would also be of interest in the future. Having in mind that remote sensing data can offer good quality information, but only on the surface layers of water, in-situ vertical optical profiles could contribute significantly to the general knowledge on the optical characteristics of the Danube Delta coastal area.

#### Acknowledgments

This work has been supported from the strategic grant POS-DRU/159/1.5/S/133391, Project “Doctoral and Post-Doctoral Programs of excellence for highly qualified human resources training for research in the field of Life Sciences, Environment and Earth Science” cofinanced by the European Social Fund within the Sectorial Operational Program Human Resources Development 2007–2013.

A part of the work has been conducted by Sorin Constantin during his four-months stay at the Laboratoire d’Océanographie de Villefranche (UMR 7093, CNRS/UPMC) in France.

Remote sensing information: NASA Ocean Biology (OB.DAAC). MODIS Ocean Color Data. Accessed on 2015/03/25.

We would like to thank the two anonymous reviewers and also Nathan Briggs for their very useful comments and suggestions.

#### References

- C.W. Anderson, 2005. USGS Handbook for Water-Resources Investigations. Chapter 6-Field Measurement. Section 6.7-Turbidity. Available online at [http://water.usgs.gov/owq/FieldManual/Chapter6/Ch6\\_contents.html](http://water.usgs.gov/owq/FieldManual/Chapter6/Ch6_contents.html).
- Bondar C., Borcia C., Radulescu C., 2011. Aspects on the extreme phenomena in Danube Mouths Area and in the Black Sea Coastal Area. In: Proceedings of the Annual Scientific Conference INHGA. pp. 209–228.
- Bondar, C., Panin, N., 2001. The Danube Delta hydrologic database and modelling. Geo-Eco-Marine 5–6, 5–52.
- Budileanu, M., 2013. Evolutia gurii de varsare Sulina pe baza modelelor numerice batimetriche. PhD thesis, University of Bucharest, Faculty of Geography (in manuscript).
- Chen, Z., Hu, C., Muller-Karger, F., 2007. Monitoring turbidity in Tampa Bay using MODIS/Aqua 250-m imagery. Remote Sens. Env. 109, 207–220. <http://dx.doi.org/10.1016/j.rse.2006.12.019>.
- Constantinescu, Ţ., Giosan, L., Vespremeanu-Stroe, a, 2010. A cartographical

- perspective to the engineering works at the Sulina mouth, the Danube Delta. *Acta Geod. Geophys Hung.* 45, 71–79. <http://dx.doi.org/10.1556/Ageod.45.2010.1.11>.
- Dinu, I., Bajo, M., Umgieser, G., Stănică, A., 2011. Influence of wind and freshwater on the current circulation along the Romanian Black Sea coast. *Geo-Eco-Marina* 17, 13–26.
- Dogliotti, A.I., Ruddick, K.G., Nechad, B., Doxaran, D., Knaeps, E., 2015. A single algorithm to retrieve turbidity from remotely-sensed data in all coastal and estuarine waters. *Remote. Sens. Environ.* 156, 157–168. <http://dx.doi.org/10.1016/j.rse.2014.09.020>.
- Doron, M., Bélanger, S., Doxaran, D., Babin, M., 2011. Spectral variations in the near-infrared ocean reflectance. *Remote. Sens. Environ.* 115 (7), 1617–1631.
- Doxaran, D., Froidefond, J., Castaing, P., 2002. A reflectance band ratio used to estimate suspended matter concentrations in sediment-dominated coastal waters. *Int. J. Remote. Sens.* 23, 5079–5085.
- Doxaran, D., Castaing, P., Lavender, S.J., 2006. Monitoring the maximum turbidity zone and detecting fine-scale turbidity features in the Gironde estuary using high spatial resolution satellite sensor (SPOT HRV, Landsat ETM+) data. *Int. J. Remote Sens.* 27, 2303–2321. <http://dx.doi.org/10.1080/0143160500396865>.
- Doxaran, D., Cherukuru, N., Lavender, S.J., 2006. Apparent and inherent optical properties of turbid estuarine waters: measurements, empirical quantification relationships, and modeling. *Appl. Opt.* 45, 2310–2324.
- Doxaran, D., Froidefond, J.M., Castaing, P., Babin, M., 2009. Dynamics of the turbidity maximum zone in a macrotidal estuary (the Gironde, France): Observations from field and MODIS satellite data. *Estuar. Coast. Shelf Sci.* 81, 321–332. <http://dx.doi.org/10.1016/j.ecss.2008.11.013>.
- European Union, 2008. Directive 2008/56/EC of the European Parliament and of the Council of 17 June 2008 establishing a framework for community action in the field of marine environmental policy (Marine Strategy Framework Directive). *Off. J. Eur. Union* 164, 19–40.
- Franz, B., 2006. Extension of MODIS Ocean Processing Capabilities to Include the 250 & 500-meter Land/Cloud Bands [WWW Document]. NASA Ocean Biol Process. Gr. 2006.URL:[http://oceancolor.gsfc.nasa.gov/DOCS/modis\\_hires/](http://oceancolor.gsfc.nasa.gov/DOCS/modis_hires/).
- Franz, B., Kwiatowska, E.J., Meister, G., McClain, C.R., 2008. Moderate Resolution Imaging Spectroradiometer on Terra: limitations for ocean color applications. *J. Appl. Remote. Sens.* 2, 023525. <http://dx.doi.org/10.1117/1.2957964>.
- Gattuso, J.-P., Smith, S.V., 2007. Coastal zone. In: Cleveland, C.J. (Ed.), 2007. *Encyclopedia of Earth*, Washington D. C., Environmental Information Coalition, National Council for Science and the Environment.
- Giosan, L., 1998. Long term sediment dynamics on Danube delta coast. in: Dronkers, J. and M.B.A.M. Scheffers (eds), *Physics of estuaries and coastal seas: proceedings of the 8th International Biennial Conference on Physics of Estuaries and Coastal Seas*, the Hague, Netherlands, 9–12 September 1996; A.A. Balkema, 365–376.
- Giosan, L., Bokuniewicz, H., Panin, N., Postolache, I., 1999. Longshore sediment transport pattern along the Romanian Danube Delta Coast. *J. Coast. Res.* 15, 859–871.
- Giosan, L., Constantinescu, S., Filip, F., Deng, B., 2013. Maintenance of large deltas through channelization: Nature vs humans Danub delta. *Anthropocene* 1, 35–45. <http://dx.doi.org/10.1016/j.ancene.2013.09.001>.
- Giosan, L., Syvitski, J., Constantinescu, S., Day, J., 2014. Protect the world's deltas. *Nature* 516, 31–33.
- Gohin, F., 2011. Annual cycles of chlorophyll-a, non-algal suspended particulate matter, and turbidity observed from space and in-situ in coastal waters. *Ocean Sci.* 7, 705–732. <http://dx.doi.org/10.5194/os-7-705-2011>.
- Gordon, H.R., Wang, M., 1994. Retrieval of water-leaving radiance and aerosol optical thickness over the oceans with SeaWiFS: a preliminary algorithm. *Appl. Opt.* 33, 443–452. <http://dx.doi.org/10.1364/AO.33.000443>.
- Goyens, C., Jamet, C., Schroeder, T., 2013. Evaluation of four atmospheric correction algorithms for MODIS-Aqua images over contrasted coastal waters. *Remote. Sens. Environ.* 131, 63–75.
- Güttler, F.N., Niculescu, S., Gohin, F., 2013. Turbidity retrieval and monitoring of Danube Delta waters using multi-sensor optical remote sensing data: An integrated view from the delta plain lakes to the western–northwestern Black Sea coastal zone. *Remote Sens. Env.* 132, 86–101. <http://dx.doi.org/10.1016/j.rse.2013.01.009>.
- IOCCG, 2000. Report 3-Remote Sensing of Ocean Colour in Coastal and Other Optically-Complex Waters.
- Kemker, C., 2014. Turbidity, Total Suspended Solids and Water Clarity. Fundamentals of Environmental Measurements. Fondriest Environmental, Web. <http://www.fondriest.com/environmental-measurements/parameters/water-quality/turbidity-total-suspended-solids-water-clarity/>.
- Knaeps, E., Raymaekers, D., Sterckx, S., Ruddick, K., Dogliotti, A.I., 2012. In-situ evidence of non-zero reflectance in the OLCI 1020 nm band for a turbid estuary. *Remote Sens. Environ.* Sentin. Spec. Issue 120, 133–144.
- Koblenz-Mishke, O.J., Volkovinsky, V.V., Kabanova, J.G., 1970. Plankton primary production of the world ocean. In: Wooster, W.S. (Ed.), *Natl. Acad. Sci. Scientific Exploration of the South Pacific*, Washington, pp. 183–193.
- McCarney-Castle, K., Voulgaris, G., Kettner, A.J., Giosan, L., 2012. Simulating fluvial fluxes in the Danube watershed: The 'Little Ice Age' versus modern day. *Holocene* 22, 91–105.
- Miller, R.L., McKee, B.A., 2004. Using MODIS Terra 250 m imagery to map concentrations of total suspended matter in coastal waters. *Remote Sens. Environ.* 93, 259–266. <http://dx.doi.org/10.1016/j.rse.2004.07.012>.
- Mobley, C.D., 1999. Estimation of the remote-sensing reflectance from above-surface measurements. *Appl. Opt.* 38 (36), 7442–7455.
- Morel, A., 1980. In-Water and Remote Measurement of Ocean Color. *Bound. Layer Meteorol.* 18, 177–201.
- Morel, A., Prieur, L., 1977. Analysis of variations in ocean color. *Limnol. Ocean.* 22, 709–722. <http://dx.doi.org/10.4319/lo.1977.22.4.0709>.
- Nechad, B., Ruddick, K.G., Neukermans, G., 2009. Calibration and validation of a generic multisensor algorithm for mapping of turbidity in coastal waters. *Remote. Sens. Ocean Sea Ice Large Water Reg.* 7473. <http://dx.doi.org/10.1117/12.830700>.
- Nechad, B., Ruddick, K.G., Park, Y., 2010. Calibration and validation of a generic multisensor algorithm for mapping of total suspended matter in turbid waters. *Remote. Sens. Env.* 114, 854–866. <http://dx.doi.org/10.1016/j.rse.2009.11.022>.
- Ouillon, S., Douillet, P., Petrenko, A., Neveux, J., Dupouy, C., Froidefond, J.M., Andréfouët, S., Muñoz-Caravaca, A., 2008. Optical algorithms at satellite wavelengths for total suspended matter in tropical coastal waters. *Sensors* 8, 4165–4185. <http://dx.doi.org/10.3390/s0874165>.
- Ovejanu, I., 2012. Morfologia și morfogeneza gurii de vărsare Sfântu Gheorghe (Delta Dunării). București: Editura Universitară, pp. 110.
- Panin, N., Jipa, D.C., Gomoiu, M.T., Scireriu, D., 1998. *Importance of sedimentary processes in environmental changes: Lower River Danube – Danube Delta – Western Black Sea System*. In: Iunilata, U. (Ed.), *Environmental Degradation of the Black Sea: Challenges and Remedies*. Kluwer Academic Publishers, Dordrecht.
- Petus, C., Chust, G., Gohin, F., Doxaran, D., Froidefond, J.-M., Sagarmiaga, Y., 2010. Estimating turbidity and total suspended matter in the Adour River plume (South Bay of Biscay) using MODIS 250-m imagery. *Cont. Shelf Res.* 30, 379–392.
- Petus, C., Marieu, V., Novoa, S., Chust, G., Bruneau, N., Froidefond, J., 2014. Monitoring spatio-temporal variability of the Adour River turbid plume (Bay of Biscay, France) with MODIS 250-m imagery. *Cont. Shelf Res.* 74, 35–49. <http://dx.doi.org/10.1016/j.csr.2013.11.011>.
- Popa, A., 1993. Liquid and sediment inputs of the Danube River into the north-western Black Sea. In: Kempe, S., Eisma, D., Degens, E.T. (Eds.), *Transport of Carbon and Nutrients in Lakes and Estuaries*, part 6 vol 74. Mitteilungen aus dem Geologisch-Palaontologischen Institut und Museum der Universität, Hamburg, pp. 137–149. SCOPE/UNEP Sonderheft, pp.
- Ruddick, K.G., Ovidio, F., Rijkeboer, M., 2000. Atmospheric correction of SeaWiFS imagery for turbid coastal and inland waters. *Appl. Opt.* 39, 897–912. <http://dx.doi.org/10.1364/AO.42.000893>.
- Ruddick, K., Park, Y., Nechad, B., 2003. MERIS imagery of Belgian coastal waters: mapping of suspended particulate matter and Chlorophyll-A. In: Proceedings of the MERIS Users Work, Frascati. ESA Spec. Publ. Sp.-549.
- Ruddick, K.G., De Cauwer, V., Park, Y.-J., Moore, G., 2006. Seaborne measurements of near infrared water-leaving reflectance: The similarity spectrum for turbid waters. *Limnol. Ocean.* 51, 1167–1179. <http://dx.doi.org/10.4319/lo.2006.51.2.1167>.
- Shen, F., Verhoeef, W., Zhou, Y., Salama, M.S., Liu, X., 2010. Satellite estimates of wide-range suspended sediment concentrations in Changjiang (Yantze) estuary using MERIS data. *Estuaries Coasts* 33 (6), 1420–1429.
- Shi, W., Wang, M., 2007. Detection of turbid waters and absorbing aerosols for the MODIS ocean color data processing. *Remote Sens. Env.* 110, 149–161. <http://dx.doi.org/10.1016/j.rse.2007.02.013>.
- Sorokin, Yu. I., 1983. The Black Sea. In: Ketchum, B.H. (Ed.), *Estuaries and Enclosed Seas. Ecosystems of the World*. Elsevier, Amsterdam, pp. 253–292.
- Stanev, E.V., Kandilarov, R., 2012. Sediment dynamics in the Black Sea: numerical modelling and remote sensing observations. *Ocean Dyn.* 62, 533–553. <http://dx.doi.org/10.1007/s10236-012-0520-1>.
- Stanica, A., Panin, N., 2009. Present Evolution and Future Predictions for the Deltaic Coastal Zone between the Sulina and Sf. 107. *Georghe Danube river mouths (Romania)*, *Geomorphology*, pp. 41–46.
- Sur, H. İ., Özsoy, E., Ilyin, Y.P., Ünlüata, Ü., 1996. Coastal/deep ocean interactions in the Black Sea and their ecological/environmental impacts. *J. Marine Syst.* 7, 293–320. [http://dx.doi.org/10.1016/0924-7963\(95\)00030-5](http://dx.doi.org/10.1016/0924-7963(95)00030-5).
- Tumanseva, N.I., 1985. *Oceanology* 25, 99–101.
- Vermote, E.F., Kotchenova, S., 2008. Atmospheric correction for the monitoring of land surfaces. *J. Geophys. Res. Atmos.* 113, 1–12. <http://dx.doi.org/10.1029/2007JD009662>.
- S.-A. Vespremeanu, 2007. *Järmul Deltei Dunării. Studiu de geomorfologie*. București: Editura Universitară, pp. 226.
- Vidraçu, I.G., 1921. Valorificarea regiunii inundabile a Dunărei. București: Tipografia URBANA.
- Wang, M., Shi, W., 2007. The NIR-SWIR combined atmospheric correction approach for MODIS ocean color data processing. *Opt. Express* 15, 15722–15733. <http://dx.doi.org/10.1029/2004JD004950>.
- Wright, L.D., 1977. Sediment transport and deposition at river mouths: a synthesis. *Geol. Soc. Am. Bull.* 88 (6), 857–868. <http://oceancolor.gsfc.nasa.gov>.